

# GABA-ergic inhibition in human hMT+ predicts visuo-spatial intelligence mediated through the frontal cortex

Reviewed Preprint

v2 • July 29, 2024

Revised by authors

Reviewed Preprint

v1 • May 17, 2024

Yuan Gao, Yong-Chun Cai, Dong-Yu Liu, Juan Yu, Jue Wang, Ming Li, Bin Xu, Teng-Fei Wang, Gang Chen, Georg Northoff , Ruiliang Bai , Xue Mei Song 

Department of Neurosurgery of the Second Affiliated Hospital and Interdisciplinary Institute of Neuroscience and Technology, Zhejiang University School of Medicine, Hangzhou 310029, China • Department of Psychology and Behavioral Sciences, Zhejiang University, Hangzhou 310028, China • Key Laboratory of Biomedical Engineering of Ministry of Education, Qiushi Academy for Advanced Studies, College of Biomedical Engineering and Instrument Science, Zhejiang University, Hangzhou 310027, China • College of Intelligence Science and Technology, National University of Defense Technology, Changsha 410073, China • Affiliated Mental Health Center & Hangzhou Seventh People's Hospital, Zhejiang University School of Medicine, Hangzhou 310013, China • University of Ottawa Institute of Mental Health Research, University of Ottawa; Ottawa, ON, K1Z 7K4, Canada • MOE Frontier Science Center for Brain Science & Brain-Machine Integration, Zhejiang University, Hangzhou 311121, China

 [https://en.wikipedia.org/wiki/Open\\_access](https://en.wikipedia.org/wiki/Open_access)

 Copyright information

## Abstract

The prevailing opinion emphasizes fronto-parietal network (FPN) is key in mediating general fluid intelligence (gF). Meanwhile, recent studies show that human MT complex (hMT+), located at the occipito-temporal border and involved in 3D perception processing, also plays a key role in gF. However, the underlying mechanism is not clear, yet. To investigate this issue, our study targets visuo-spatial intelligence, which is considered to have high loading on gF. We use ultra-high field magnetic resonance spectroscopy (MRS) to measure GABA/glutamate concentrations in hMT+ combined with resting-state fMRI functional connectivity (FC), behavioral examinations including hMT+ perception suppression test, and a gF subtest for its visuo-spatial component. Our findings show that both GABA in hMT+ and frontal-hMT+ functional connectivity significantly correlate with the performance of visuo-spatial intelligence. Further, serial mediation model demonstrates that the effect of hMT+ GABA on visuo-spatial gF is fully mediated by the hMT+ frontal FC. Together, our findings highlight the importance in integrating sensory and frontal cortices in mediating the visuospatial component of general fluid intelligence.

### eLife assessment

This study employed a comprehensive approach to examining how the MT+ region integrates into a complex cognition system in mediating human visuo-spatial intelligence. While the findings are **useful**, the experimental evidence is **incomplete** and the study designs, hypotheses, and data analyses need to be improved. The work will be of interest to researchers in psychology, cognitive science, and neuroscience.

<https://doi.org/10.7554/eLife.97545.2.sa3>

## Introduction

General fluid intelligence (gF) is a current problem-solving ability, which shows high inter-individual differences in humans (Cattell & Raymond, 1963). At the beginning of the last century, Spearman (Spearman, 1904) proposed that some general or g factor contributes to our gF. One key component of gF is visuo-spatial intelligence that, usually tested by visual materials, shows high g-loading (Colom et al., 2006; Deary et al., 2010; Jung & Haier, 2007). The exact neural mechanisms of the interplay of visuo spatial intelligence with gF remain yet unclear, though.

The “neuro-efficiency” hypothesis is one explanation for individual differences in gF (Haier et al., 1988). This hypothesis puts forward that the human brain’s ability to suppress irrelevant information leads to more efficient cognitive processing. Correspondingly, using a well-known visual motion paradigm (center-surround antagonism) (Liu et al., 2016; Tadin et al., 2003), Melnick et al found a strong link between suppression index (SI) of motion perception and the scores of the block design test (BDT, a subtest of the Wechsler Adult Intelligence Scale (WAIS), which measures the visuo-spatial component (3D domain) of gF (Melnick et al., 2013). Motion surround suppression (SI), a specific function of human extrastriate cortical region, middle temporal complex (hMT+), aligns closely with this region’s activities (Gautama & Van Hulle, 2001). Furthermore, hMT+ is a sensory cortex involved in visual perception processing (3D domain) (Cumming & DeAngelis, 2001). These findings suggest that hMT+ potentially plays a significant role in 3D visuo-spatial gF by facilitating the efficient processing of 3D visual information and suppressing irrelevant information. However, more evidence is needed to uncover how the hMT+ functions as a core region for 3D visuo-spatial intelligence. We here hypothesize a key role of hMT+ GABA and its functional connectivity with the frontal cortex in mediating visuospatial gF (Figure 1a).

To investigate our hypothesis, this work conducted multi-level examination including biochemical (Glutamatergic - GABAergic in hMT+), regional-systemic (brain connectivity with hMT+ - based), and behavioral (visual motion function in hMT+) levels to reveal if hMT+ contributes to the 3D visuo-spatial component of gF. We employ ultra-high field (7T) magnetic resonance spectroscopy (MRS) technology to reliably resolve GABA and Glu concentrations (Ende, 2015; Liu et al., 2022; Song et al., 2021). To verify the specificity of hMT+, we used primary visual cortex (V1) - based GABA/Glu as control as it mediates the 2D rather than 3D visual domain (Cumming & DeAngelis, 2001).

Our findings first demonstrate that GABAergic inhibition mechanisms (but not excitatory Glu) in hMT+ region relate to 3D visuo-spatial ability. Further, analysis of functional brain connectivity at rest reveals that the network (between hMT+ and frontal cortex) relating to hMT+ GABA and perceptual suppression contribute to visuo-spatial gF. Our results provide direct evidence that GABA-ergic inhibitory mechanisms in hMT+ region (a sensory cortex) mediate the multi-level visuo-spatial component (3D domain) of gF thus drawing a direct connection of biochemistry, brain connectivity, and behavior.

## Results

To determine whether the function of hMT+ cortex contributes to visuo-spatial component (3D domain) of gF, we adopted the experimental design depicted in Figure 1b. Thirty-six healthy subjects participated in this study. Participants underwent two MRI sessions: the first encompassing resting-state fMRI and magnetic resonance spectra (MRS), and the second solely involving MRS. A 30-minute interval separated these sessions, during which participants

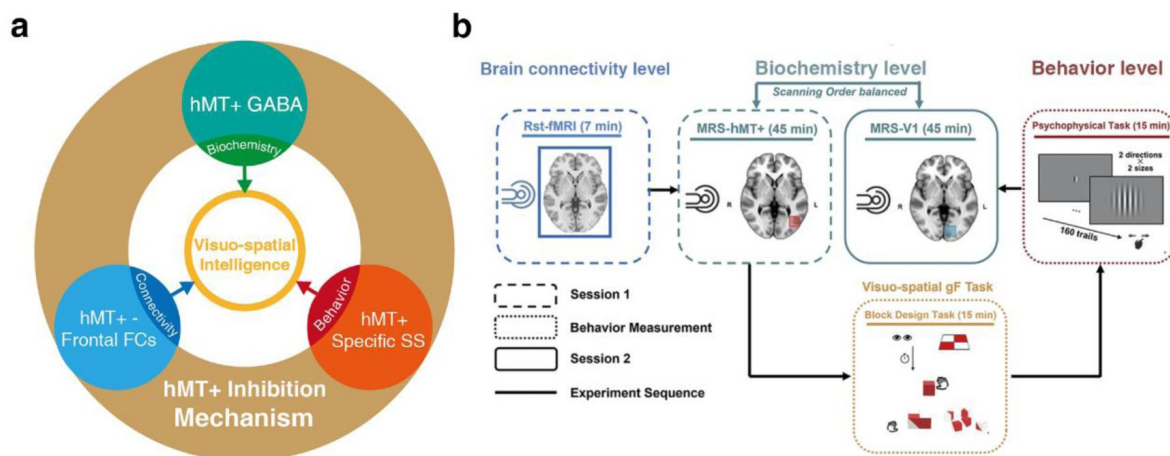


**Figure 1.**

Hypothesis and experimental design. **(a)** Schematic of hypothesis. The inhibition mechanism centered on hMT+, including the molecular level: the GABAergic inhibition in hMT+ (green circle), brain connectivity level: hMT+ - frontal functional connectivity (blue circle), and behavior level: hMT+ specific surround suppression of visual motion (red circle), contributes to the visuo-spatial component of gF (3D domain, yellow circle). **(b)** Schematic of experimental design. Session 1 (rectangle box of short line) was the functional MRI and MRS scanning at resting state. Session 2 (rectangle box of solid line) was another region of MRS acquisition. In the two sessions, the order of MRS scanning regions (hMT+ and V1) was counter balanced across participants. There was a structural MRI scanning before each MRS data acquisition. The interval between the two sessions was used for behavioral measurement (rectangle box of dotted line): block design task (BDT) and psychophysical task - motion discrimination. Solid lines indicate the experiment sequence.

performed motion discrimination tasks (using center-surround antagonism stimuli) (Tadin et al., 2003) and the block design test (BDT), which assesses the visuo-spatial ability (3D domain) of gF (Fangmeier et al., 2006). In the motion discrimination tasks, a grating of either large or small size was randomly presented at the center of the screen. The grating drifted either leftward or rightward, and participants were asked to judge the perceived moving direction. While in the Block design test, participants were asked to rebuild the figural pattern within a specified time limit using a set of red and white blocks. Both the volume-of-interests (VOIs) of MRS scanning in the left hMT+ (targeted brain area) and the left primary visual cortex (V1, control brain area) had dimensions of  $2 \times 2 \times 2 \text{ cm}^3$ , with the MRS scanning sequences being randomized across the two MRS sessions. The hMT+ MRS VOIs were demarcated using an anatomical landmark (Dumoulin et al., 2000). For 14 subjects, we also utilized fMRI to functionally pinpoint the hMT+ to validate the placement of the VOI (Figure 2a, b). The V1 MRS VOIs were anatomically defined (Methods). Here, MRS data after extensive quality control (31/36 in hMT+, and 28/36 in V1) were taken for further analysis (Methods).

## GABA and Glu concentrations in hMT+ and V1 and their relation to SI and BDT

An example of a MRS voxel located in hMT+ is shown in Figure 3a. LCModel fittings for GABA spectra from all subjects in hMT+ ( $n = 31$ ) and V1 ( $n = 28$ ) are illustrated in Figure 3b (color scale presents the BDT scores). We discerned a significant association between the inter-subjects' BDT scores and the GABA levels in hMT+ voxels, but not in V1 voxels. Quantitative analysis displayed that BDT significantly correlates with GABA concentrations in hMT+ voxels ( $r = 0.39$ ,  $P = 0.03$ ,  $n = 31$ , Figure 3c). After using partial correlation to control for the effect of age, the relationship remains significant ( $r_{\text{partial}} = 0.43$ ,  $P = 0.02$ , 1 participant excluded due to the age greater than mean + 2.5SD). In contrast, there was no correlation between BDT and GABA levels in V1 voxels (figure supplement 1a). Further, we show that SI significantly correlates with GABA levels in hMT+ voxels ( $r = 0.44$ ,  $P = 0.01$ ,  $n = 31$ , Figure 3d). In contrast, no significant correlation between SI and GABA concentrations in V1 voxels was observed (figure supplement 1b). This finding is in line with prior results, which indicates that motion perception is associated with neural activity in hMT+ area, but not in V1 (Schallmo et al., 2018). LCModel fittings for Glu spectra from all subjects in hMT+ ( $n = 31$ ) and V1 ( $n = 28$ ) voxels are presented in figure supplement 2a.

Unlike in the case of GABA, no significant correlations between BDT and Glu levels were found in both hMT+ and V1 voxels (figure supplement 2b, c). While, as expected (Song et al., 2021), we observed significant positive correlations between GABA and Glu concentrations in both hMT+ ( $r = 0.62$ ,  $P < 0.001$ ,  $n = 31$ ) and V1 voxels ( $r = 0.56$ ,  $P = 0.002$ ,  $n = 28$ ) (figure supplement 3a, b). Additionally, significant correlations between SI and BDT, small threshold and SI were discerned ( $r = 0.59$ ,  $P = 0.0002$ ,  $n = 34$ , figure 3e,  $r_{\text{partial}} = 0.67$ ,  $P < 0.001$ , 1 participant excluded due to the age greater than mean + 2.5SD;  $r = -0.43$ ,  $P = 0.016$ ,  $r_{\text{partial}} = 0.44$ ,  $P = 0.014$ ). While there was no significant correlation between large threshold and SI, corroborating previous conclusions (Melnick et al., 2013). Two outliers evident in Figure 3e were excluded, with consistent results depicted in figure supplement 4a. Further, two outliers evident in Figure 3d were excluded, with consistent results depicted in figure supplement 4b.

## MT - frontal FC relates to SI and BDT

We next took the left hMT+ as the seed region and separately measured interregional FCs between the seed region and each voxel in the frontal regions (a priori search space). These measurements were correlated with the performance in 3D visuospatial ability (BDT) to identify FCs with significant correlations. Results from connectivity-BDT analysis are summarized in Table 1 and shown in Figure 4a. We found that brain regions with high FC strength to the seed region (left hMT+) significantly correlated with BDT scores, these included mainly regions situated within the canonical cognitive cores of FPN (Brodmann areas (BAs) 6, 9, 10, 46, 47) (Assem et al., 2020);

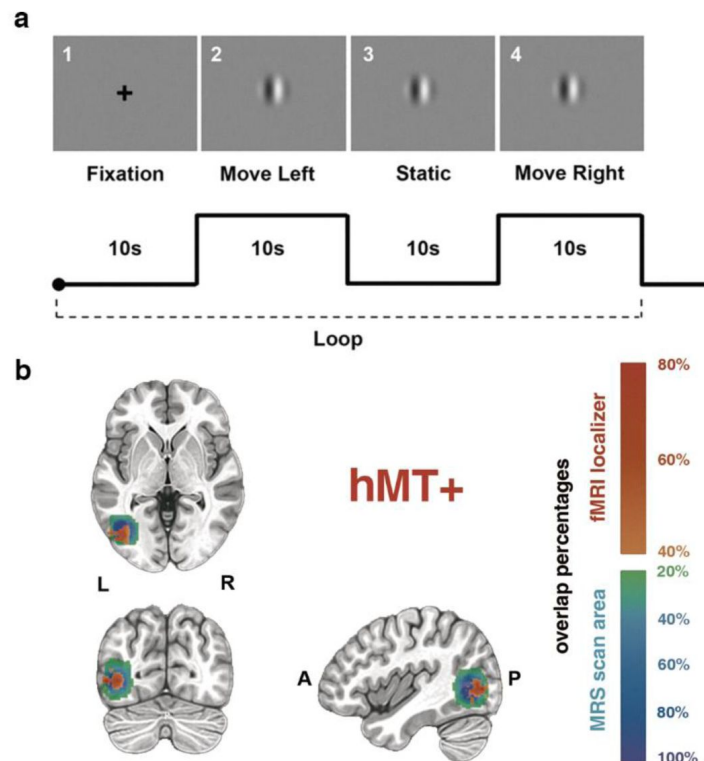


**Figure 2.**

hMT+ localizer scans and hMT+ MRS VOI placement. **(a)** Single task block designs. First: a cross fixation on the center of the screen (10s). Second: a moving grating ( $2^\circ$ ) toward left last 10s. Third: the grating keeps static for 10s. Fourth: the grating moves toward right last 10s. The localizer scans consist of 8 blocks. **(b)** hMT+ location and MRS VOI placement. The upper template is the horizontal view. The lower templates from left to right are coronal and sagittal views. The warm color indicates the overlap of fMRI activation of hMT+ across 14 subjects, the cold color bar indicates the overlap of MRS VOIs across all subjects.

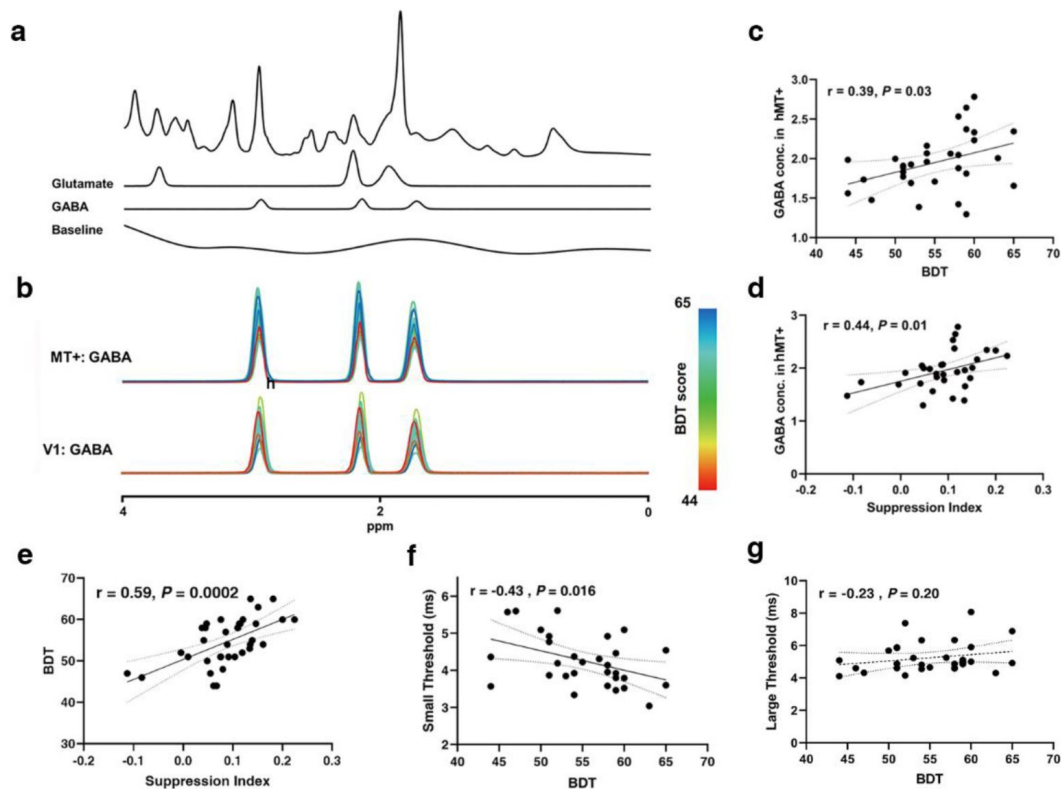


**Figure 3.**

MRS spectra and the relationships between GABA levels and SI / BDT. **(a)** Example spectrum from the hMT+ voxel of one participant. The first line is the LCModel fitting result of all metabolites, and the following lines show the Glu and GABA spectra fitting with LCModel, and then the baseline. **(b)** Individual participants fitted GABA MRS spectra from the hMT+ (top) and V1 (bottom) voxels from baseline measurement. The colors of the GABA spectra represent the individual differences of BDT. The color bar represents the scores of BDT. **(c) and (d)** Pearson's correlations showing significant positive correlations between hMT+ GABA and BDT scores **(c)**, between hMT+ GABA and SI **(d)**. GABA and Glu concentrations (Conc.) are absolute, with units of mmol per kg wet weight (Methods). **(e)** Pearson's correlation showing significant positive correlations between SI and BDT. **(f)** Pearson's correlation showing significant negative correlations between BDT and small threshold. **(g)** No correlation between BDT and large threshold. The ribbon between dotted lines represents the 95% confidence interval, and the black regression line represents the Pearson's correlation coefficient ( $r$ ).



Deary et al., 2010 [↗](#); Duncan et al., 2020 [↗](#); Duncan et al., 2000 [↗](#); Gray et al., 2003 [↗](#); Jung & Haier, 2007 [↗](#)). Across the whole brain search, the similar FCs (between hMT+ and frontal cognitive cores) still showed significant correlations with BDT scores (Table supplement 1) (also shown in **figure supplement 5a** [↗](#)). Additionally, we identified certain parietal regions (BAs 7, 39, 40) with significant correlations of their functional connectivity to the left hMT+ and the BDT scores (Table supplement 1) (also shown in **figure supplement 5a** [↗](#)). These significant connections between hMT+ and FPN system suggest that left hMT+ is involved in the efficient information integration network mediating the visuo spatial component of gF.

To address the question whether spatial suppression plays a role, we correlated hMT+ - based global FCs with SI. Though spatial suppression during motion perception (quantified by SI) is considered to be the function of area hMT (Gautama & Van Hulle, 2001 [↗](#)), the top-down modulation from the frontal cortex can increase surround suppression (Liu et al., 2016 [↗](#)). Our functional connectivity-SI analysis in the frontal regions (a priori search space) displayed 3 brain regions in which FCs strength significantly correlated with SI: right BA4/6, left BA6, and right BA46 (summarized in Table supplement 2, and shown in **Figure 4b** [↗](#)). Across the whole brain search, we identified total 7 brain regions in which FCs strength significantly correlated with SI, and 3 of these were in the frontal cortex. This is consistent with the results obtained by the functional connectivity-SI analysis in a priori search space (frontal cortex) (Table supplement 3 and **figure supplement 5b** [↗](#)).

## Local hMT+ GABA acts on SI and BDT via global MT-frontal connectivity

To determine whether local neurotransmitter levels (such as GABA and Glu) in the hMT+ region mediate the broader 3D visuo-spatial ability of BDT, which as a component of gF, is linked to the frontal cortex (Fangmeier et al., 2006 [↗](#)), we correlated the significant FCs of hMT+ - frontal in **Figure 4a** [↗](#) (also shown in **Table 1** [↗](#)) with the GABA and Glu levels in hMT+ region. The results revealed that only two FCs significantly correlated with inhibitory GABA levels in hMT+: 1) the FC of left hMT+ - right BA 46 (significantly negative correlation,  $r = -0.56$ ,  $P = 0.02$ ,  $n = 29$ , FDR correction, **Figure 5a** [↗](#) left); 2) the FC of left hMT+ - right BA 6 (significantly positive correlation,  $r = 0.69$ ,  $P = 0.002$ ,  $n = 29$ , FDR correction, **Figure 5b** [↗](#) left) (also shown in **Table 2** [↗](#)). There were no significant correlations between these FCs and the excitatory Glu levels in hMT+ (**Table 2** [↗](#)). Across the whole brain search, we obtained the same two hMT+ - frontal FCs significantly correlating with both hMT+ GABA levels and BDT (Table supplement 4), this is consistent with the results in the priori search space (frontal cortex) (**Table 2** [↗](#)). We then correlated the significant FCs in **Figure 5b** [↗](#) (also in Table supplement 2) with GABA and Glu concentrations in hMT+ and found that almost all the correlations are significant except one (between the FC of left hMT+ - right BA46 and the Glu levels in hMT+) (Table supplement 5). Among the three FCs, the clusters of two FCs have substantial voxel overlap with the FCs we found by the connectivity-BDT analysis (**Figure 5a** [↗](#), b). Across the whole brain search, there were total 7 brain regions in which FCs strength were significantly correlated with SI, all the 7 FCs significantly correlated the hMT+ GABA levels, while, no FC had significant correlation with the hMT+ Glu levels (Table supplement 6).

Taken together, our results displayed that the overlap FCs from the analyses of connectivity - behavior (BDT and SI) -GABA are the hMT+ - BA 46 and hMT+ - BA 6 (**Figure 5a** [↗](#), b). These results suggest that the coupling of FCs of hMT+ - frontal regions (BA 46 and BA 6) with local hMT+ GABA provides the neural basis for both the simple motion perception (quantified by SI) and the complex 3D visuo-spatial ability (quantified by BDT).

In order to fully investigate the potential roles of the multiples variables contributing to BDT scores, serial mediation analyses (Hayes, 2013 [↗](#)) were applied to both MR and behavioral data. Following our hypothesis, the independent variable (X) is hMT+ GABA, the dependent variable (Y) is BDT scores, the covariate is the age, and the mediators are FC (M1) and SI (M2). We used the

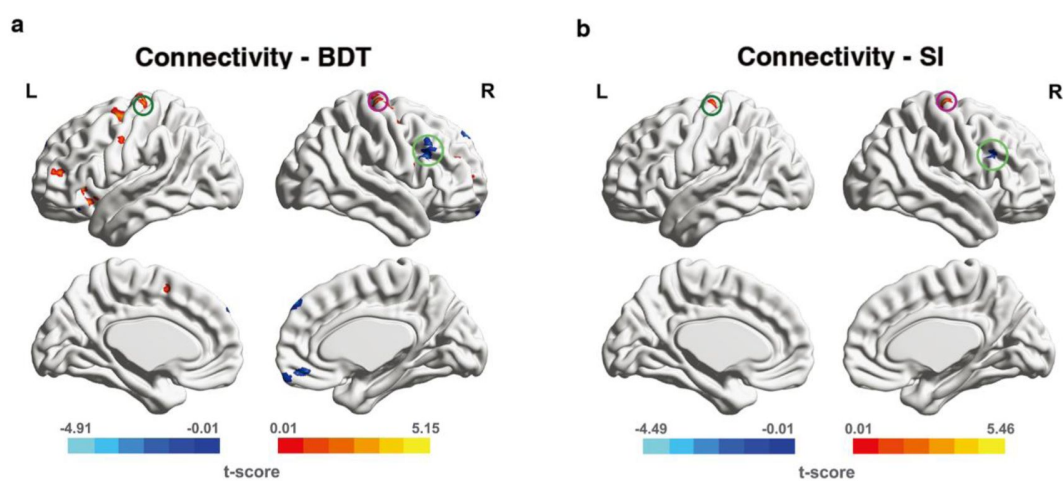


**Figure 4.**

Significant FCs from connectivity-behavior analyses in *a priori* search space. The seed region is the left hMT+. The significant FCs are obtained from *a priori* space (frontal cortex). **(a)** The significant FCs obtained from connectivity-BDT analysis. Single voxel threshold  $P < 0.005$ , adjacent size  $\geq 23$  (*AlphaSim* correcting, Methods). **(b)** The significant FCs obtained from connectivity-SI analysis. Single voxel threshold  $P < 0.005$ , adjacent size  $\geq 22$  (*AlphaSim* correcting, Methods). Positive correlations are shown in warm colors, while, negative correlations are shown in cold colors. The paired deep green, deep pink, light green circles on **(a)** and **(b)** indicate the overlap regions in left BA6, right BA6, right BA46 (DLPFC) between Connectivity - BDT analysis and Connectivity - SI analysis, respectively.



FC number	Connected regions	BA	Size	Peak coordinate	<i>r</i>	<i>P</i>
				MNI ( <i>x, y, z</i> )		
1	Frontal_Sup_Orb_R	11	33	(12,63, -19.5)	-0.57	0.0011
2	Frontal_Inf_Orb_L	47	24	(-34.5,28.5, -13.5)	-0.63	0.0003
3	Frontal_Med_Orb_R	11	41	(3,43.5, -12)	-0.58	0.0009
4	Frontal_Inf_Orb_R	47	48	(-31.5,24, -12)	0.59	0.0008
5	Frontal_Inf_Orb_R	47	29	(25.5,30, -13.5)	0.67	0.0001
6	Insula_L	\	26	(-28.5,27,0)	0.67	0.0001
7	Frontal_Inf_Oper_R	45	41	(43.5,16.5,6)	0.64	0.0002
8	Frontal_Sup_R	10	25	(31.5,57,9)	0.59	0.0008
9	Frontal_Mid_L	10	82	(-33,48,12)	0.62	0.0003
10	Frontal_Inf_Oper_R	44	49	(51,7.5,21)	0.59	0.0007
11	Frontal_Inf_Oper_R	46	96	(49.5,16.5,28.5)	-0.62	0.0003
12	Frontal_Mid_L	10	32	(-31.5,49.5,24)	0.57	0.0012
13	Frontal_Mid_R	10	102	(31.5,36,30)	0.59	0.0009
14	Precentral_L	6	46	(-49.5, -1.5,34.5)	0.59	0.0007
15	Frontal_Mid_R	9	107	(51,19.5,40.5)	-0.67	0.0001
16	Frontal_Sup_L	9	35	(-9,60,37.5)	-0.69	0.0001
17	Frontal_Sup_Medial_R	9	74	(4.5,52.5,43.5)	-0.57	0.0011
18	Frontal_Sup_R	6	136	(28.5, -7.5,63)	-0.64	0.0002
19	Supp_Motor_Area_L	6	48	(-10.5,6,54)	0.63	0.0003
20	Frontal_Mid_L	6	119	(-24,4.5,55.5)	0.63	0.0003
21	Precentral_L	6	229	(-24, -18,66)	0.60	0.0005
22	Frontal_Sup_R	6	32	(16.5, -18,67.5)	0.68	0.0001
23	Precentral_R	6	80	(30, -24,70.5)	0.70	0.0001
24	Precentral_R	6	23	(16.5, -25.5,76.5)	0.70	0.0001

Single voxel threshold  $P < 0.005$  ( $t > 3.057$  or  $t < -3.057$ ), adjacent size  $\geq 23$  voxels (AlphaSim corrected).

**Table 1**

**FC of voxels showing significant correlation with BDT scores across subjects in frontal cortex.**

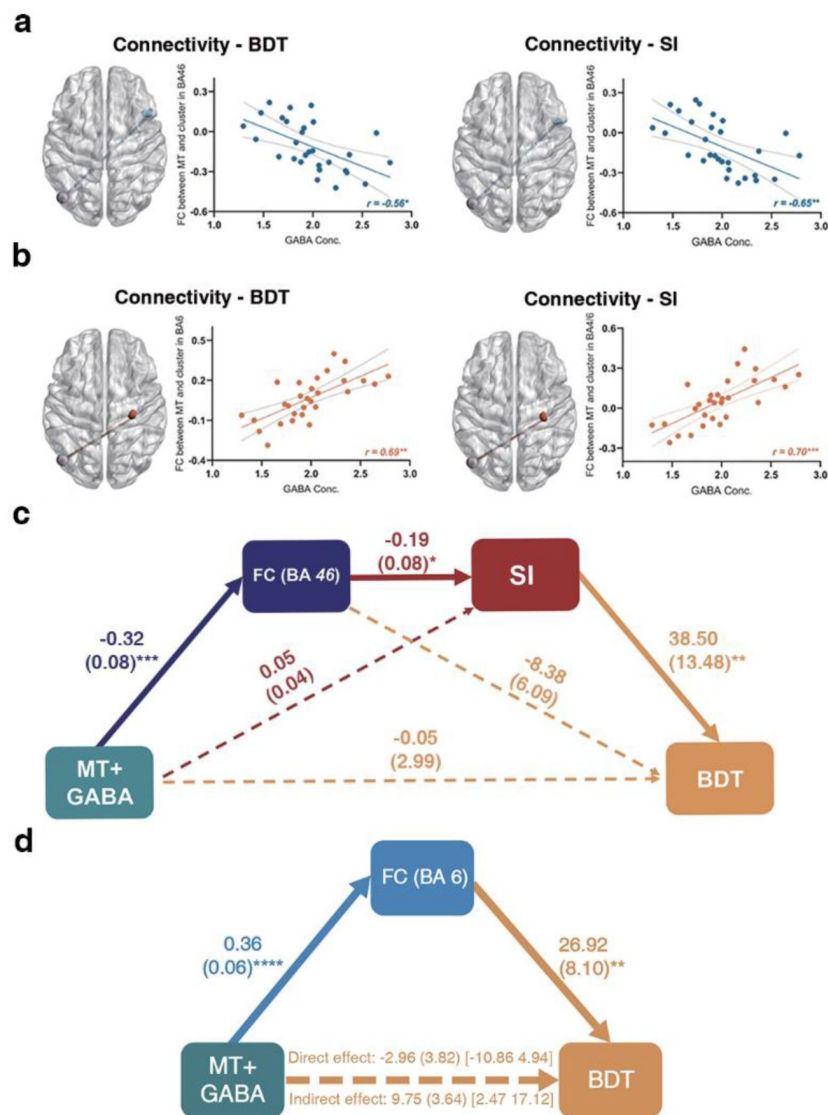


**Figure 5.**

Local hMT+ GABA acts on SI and BDT via global MT-frontal connectivity. **(a)** Significant negative correlation between the FC of left hMT+ - right DLPFC (BA46) and hMT+ GABA (*FDR* correction). **(b)** Significant positive correlation between the FC of left hMT+ - right (pre) motor cortex (BA4/6) and hMT+ GABA (*FDR* correction). In **(a)** and **(b)**, left: the significant FCs obtained from connectivity-BDT analysis; right: the significant FCs obtained from connectivity-SI analysis. **(c)** Significant pathways: hMT+ GABA → FC (left hMT+ - right BA46, negative correlation) → SI (negative correlation) → BDT (positive correlation). This pathway can explain 34% of the variance in BDT. **(d)** Significant pathways: hMT+ GABA → FC (left hMT+ - right BA6, positive correlation) → BDT (positive correlation). The bolded lines represent the hypothesized mediation effect. The dotted lines represent alternative pathways. \*:  $P < 0.05$ ; \*\*:  $P < 0.01$ ; \*\*\*:  $P < 0.001$ .

FC number	hMT+ GABA concentrations			hMT+ Glu concentrations		
	<i>r</i>	<i>P</i>	<i>FDR</i>	<i>r</i>	<i>P</i>	<i>FDR</i>
1	-0.07	0.72	0.75	-0.11	0.58	0.85
2	-0.28	0.14	0.36	-0.27	0.15	0.81
3	-0.13	0.52	0.59	-0.07	0.71	0.85
4	0.10	0.59	0.64	0.12	0.54	0.85
5	0.14	0.48	0.58	0.24	0.21	0.81
6	0.31	0.11	0.33	0.15	0.43	0.85
7	0.20	0.30	0.48	0.07	0.74	0.85
8	0.14	0.45	0.58	0.05	0.79	0.85
9	0.20	0.30	0.48	0.10	0.60	0.85
10	-0.13	0.49	0.58	-0.16	0.41	0.85
11	<b>-0.56</b>	<b>0.0018</b>	<b>0.02*</b>	-0.22	0.25	0.81
12	0.18	0.34	0.51	0.15	0.43	0.85
13	0.20	0.30	0.48	0.05	0.81	0.85
14	0.39	0.04	0.14	0.22	0.24	0.81
15	-0.40	0.03	0.12	-0.21	0.27	0.81
16	-0.27	0.15	0.36	-0.12	0.53	0.85
17	0.17	0.37	0.52	0.06	0.74	0.85
18	0.26	0.18	0.39	0.16	0.40	0.85
19	0.39	0.03	0.12	0.31	0.10	0.81
20	0.01	0.98	0.98	0.14	0.46	0.85
21	0.40	0.03	0.12	0.24	0.21	0.81
22	0.22	0.25	0.48	0.06	0.76	0.85
23	<b>0.69</b>	<b>0.0001</b>	<b>0.002**</b>	0.47	0.01	0.24
24	0.41	0.03	0.12	0.001	0.97	0.97

Bold font indicates the significant correlations survived from multi correlation correction.

**Table 2.**

**Correlations between FC in Table 1 [↗](#) and GABA/Glu concentrations in hMT+.**

overlap clusters from the analyses of connectivity-BDT-GABA and connectivity-SI-GABA to compute the FC of hMT+ - BA46, 1 participant was excluded due to his age greater than mean + 2.5SD. The serial mediation model is shown in **Figure 5c**. GABA levels in hMT+ significantly negatively correlated with the FC of hMT+ - BA46 ( $\beta = -0.32$ ,  $P < 0.001$ ), which in turn significantly negatively correlated with SI ( $\beta = -0.19$ ,  $P = 0.035$ ), and consequently, significantly positively correlated with BDT ( $\beta = 38.5$ ,  $P = 0.009$ ). Critically, bootstrapped analyses revealed that our hypothesized indirect effect (i.e., hMT+ GABA  $\rightarrow$  FC of hMT+ - BA46  $\rightarrow$  SI  $\rightarrow$  BDT) was significant ( $\beta = 2.28$ , SE = 1.54, 95% CI = [0.03, 5.94]). The model accounted for 34% of the variance in BDT. However, when considering the MT-BA6 FC as the mediator M1, the serial model does not show a significant indirect effect. Consequently, we explored a mediation model, which revealed that the MT-BA6 FC totally mediates the relationship between GABA and BDS. (**Figure 5d**). For sensitivity purposes, we tested the alternative models, in which the order of the mediators was reversed. The pathway that hMT+ GABA was predicted to be associated with SI, followed by the FC of hMT+ - BA 46, and then BDT, did not yield the chained mediation effects on BDT (**figure supplement 6**).

To summarize (shown in **Figure 6**), the results from the serial mediation analyses are consistent with our hypothesis. That is, higher GABAergic inhibition in hMT+ relates to stronger negative FC between hMT+ and BA46, leading to enhanced ability for surround suppression (filtering out irrelevant information(Tadin, 2015)), which ultimately results in more efficient visual 3D processing as key component of gF (the higher BDT scores).

## Discussion

Here, we provide evidence that hMT+ inhibitory mechanisms mediate processing in the visuo-spatial component (3D domain) of gF on multiple levels, that is, from molecular over brain connectivity to behavior. First, this study found that higher hMT+ inhibitory GABA levels (but not excitatory Glu) relate to FC between hMT+ and BA 46 that contribute to both SI and 3D visuo-spatial intelligence (BDT). Our serial mediation analyses indicate that the inhibitory mechanisms related to hMT+ and its GABA levels (but not Glu), FCs of hMT+ - BA46 coupling with hMT+ inhibitory GABA (but not excitatory Glu), and behavior (SI indexing perceptual suppression in hMT+) predict the inter-subject variance in the 3D visuo-spatial intelligence (BDT) (**Figure 5c**). Second, we demonstrate discrete GABAergic inhibition mechanisms in hMT+ that mediate the strong FCs between hMT+ - frontal regions (BA46 and BA6): significant negative correlation with the FC of hMT+ - BA 46 (**Figure 5a**), whereas there is significant positive correlation with the FC of hMT+ - BA 6 (**Figure 5b**). This indicates that different frontal regions, DLPFC (BA 46) and premotor cortex (BA6), contribute uniquely to gF through hMT+ - based inhibitory mechanisms.

The goal of our research is to reveal that the inhibitory (not excitatory) mechanism in hMT+ contributes to multi-level processing in 3D visuo-spatial ability (BDT). Monkey electrophysiological experiments revealed that selective attention gates the visual cortex, including area MT, effectively suppressing the irrelevant information(Everling et al., 2002; Treue & Maunsell, 1996). These findings align with the “neural efficiency” hypothesis of intelligence (Haier et al., 1988), which puts forward the human brain’s ability to suppress the repetition of information. Neural suppression is associated with the balance between excitation and inhibition (EIB), usually represented by covariation between Glutamate and GABA(Ozeki et al., 2009). Here, this study exploited the high spectral resolution afforded by ultrahigh field (7T) MRS to reliably resolve GABA measurement, to adequately discriminate the glutamate and glutamine signals, and to resolve the high accuracy Glu measurement(Ende, 2015). This work implemented the MRS scanning in hMT+ (3D visual domain) and V1 (2D visual domain) regions and found that hMT+ inhibitory GABA (but not excitatory Glu) significantly correlated with 3D visuo-spatial intelligence, i.e., the higher GABA levels in hMT+ (rather than excitatory Glu) relate to higher visual 3D processing (**Figure 3c**). We searched the global hMT+ - based FCs with the connectivity-BDT analyses (in priori search space and whole brain search to valid), and then, correlated these significant FCs

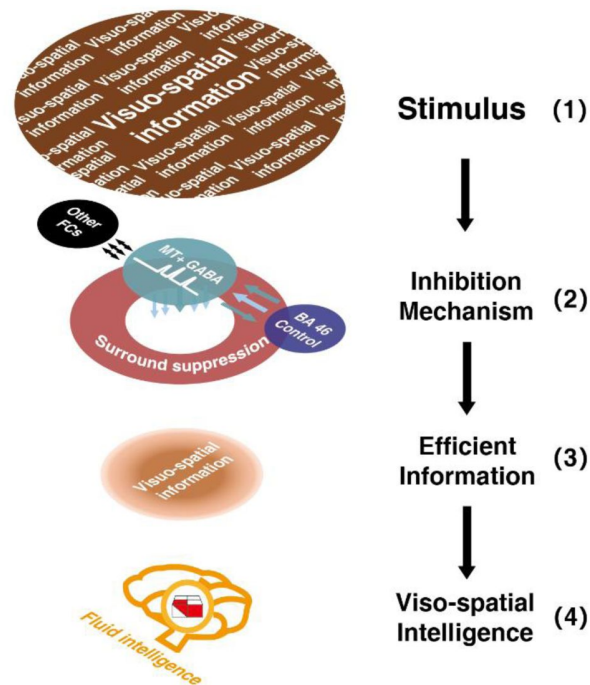


**Figure 6.**

Sketch depicting the multi-level inhibitory mechanisms centered on hMT+ GABA contributing to visuo-spatial intelligence. Inhibitory GABA in hMT+ (a sensory cortex, shown in green circle), coupling with the functional connectivity between hMT+ and BA46 (cognitive control core, shown in purple circle), and mediated by motion surround suppression (shown in red circle), contributes to visuo-spatial intelligence (BDT, 3D domain, shown in red and white building blocks). In this sketch, the two-colored parallel arrows show the negative FC between hMT+ and BA46, the colored arrows below the green circle display the inhibition mechanisms centered on hMT+ GABA (2), filtered the irrelevant information in (1) and focused on the efficient visuo-spatial information (3). Black long arrows display the direction of information flow: from input information (1) to visuo-spatial intelligence (4).

with the GABA and Glu concentrations in hMT+. We found two FCs (MT+ - BA46 and hMT+ - BA6) significantly correlating with hMT+ inhibitory GABA (whereas no FC significantly correlated with hMT+ excitatory Glu). Accordingly, our results emphasize the importance of hMT+ inhibitory GABA (but not excitatory Glu) in processing the 3D visual-spatial intelligence (BDT).

Our recent human study (Song et al., 2021 [\[1\]](#)) and other study's animal experiments (Ozeki et al., 2009 [\[2\]](#); Sato et al., 2016 [\[3\]](#)) demonstrated that the conjoint action of inhibition (GABA) and excitation (Glu) underlies visual spatial suppression. In this work, our novel data show the chained mediation effects from local hMT+ GABA to more global 3D visuo-spatial intelligence: hMT+ GABA → FC (MT+ and BA46) → SI → BDT. Thereby, our data indicate that inhibitory mechanisms in hMT+, from the biochemical level of GABA over FC to the behavioral level, can predict the inter- subject variance in the 3D visuo-spatial intelligence (BDT) (**Figure 5c** [\[4\]](#)).

Another interesting finding reveal that GABAergic inhibition in hMT+ coupling with distinct functional connectivity patterns between BA 46-MT+ and BA6-MT+. A previous human fMRI experiment found that the positive and negative correlations between 3D visuo-spatial intelligence and the activation of frontal regions appeared at different reasoning phases (validation or integration phases during reasoning) (Fangmeier et al., 2006 [\[5\]](#)). On the one hand, a monkey electrophysiological experiment reported the delayed modulation from PFC (especially in DLPFC (BA 46))) to area MT during a visual motion task (Zaksas & Pasternak, 2006 [\[6\]](#)). Computational models converged with empirical data of awake monkey experiments slowing temporal modulation from PFC to MT/MST (Donner et al., 2009 [\[7\]](#); Siegel et al., 2015 [\[8\]](#); Wang, 2002 [\[9\]](#); Wimmer et al., 2015 [\[10\]](#)). On the other hand, human MEG studies (Donner et al., 2009 [\[7\]](#); Wilming et al., 2020 [\[11\]](#)) reported that gamma-band activity in visual cortex (including area MT) exhibits high coherence with the activity in (pre-) motor regions (BA 4/6). These results suggest that the relation of long-range FC and local inhibitory mechanism (MT+ GABA) support our findings that inhibitory GABA in hMT+ contributes to efficient long-range integration and coordination in distant brain areas like the prefrontal and premotor cortex.

How does hMT+ functions as a core region for 3D visuo-spatial intelligence. rather than as simple input module? The results in **Figure 5a** [\[4\]](#), c showed that the overlap brain regions from the analyses of connectivity-BDT-GABA/connectivity-SI-GABA are the hMT+ - BA 46. This overlap couples with local visual suppression (SI) and consequently plays an important role in 3D visuo-spatial intelligence. The direction discrimination task in this work (the visual motion paradigm of center-surround antagonism) was previously considered a mainly local function of hMT+ (Melnick et al., 2013 [\[12\]](#); Tadin, 2015 [\[13\]](#); Tadin et al., 2003 [\[14\]](#)). However, our results with connectivity-SI analyses revealed that both local (FC within BA 18) and global brain connectivity (FC between hMT+ and frontal regions) contribute to SI (Table supplement 3). In human psychophysical experiments (Melnick et al., 2013 [\[12\]](#); Tadin et al., 2003 [\[14\]](#)) the brief stimulus duration (~100 ms) in motion discrimination precludes most top-down attentional feedback effects (Wang, 2002 [\[9\]](#); Zaksas & Pasternak, 2006 [\[6\]](#)), while, attention, which predicted the performance of the motion discrimination task, was sustained throughout the stimulus intervals (Siegel et al., 2015 [\[8\]](#)). Furthermore, animal experiments have revealed that the local circuits in the visual cortex combining with top-down modulation and intracortical horizontal connection mediate the visual-spatial suppression (Angelucci et al., 2002 [\[15\]](#); Keller et al., 2020 [\[16\]](#); Li et al., 2019 [\[17\]](#); Zhang et al., 2014 [\[18\]](#)).

Our results (shown in **Figure 5a** [\[4\]](#), b, right) present the intrinsic binding of local GABAergic inhibition in hMT+, which suppressing redundancy of visual motion processing (SI), and the activity of brain connectivity between hMT+ and frontal regions. These individually inherent traits may contribute to the individual difference in 3D visuo-spatial ability (**Figure 5a** [\[4\]](#), b, left). A candidate divisive normalization model (Carandini & Heeger, 2011 [\[19\]](#); Reynolds & Heeger, 2009 [\[20\]](#))



can explain how such reverberation affects the process of suppressing the irrelevant information, from perception to intelligence (Melnick et al., 2013; Tadin, 2015). We summarize a framework (Figure 6) to indicate and visualize our findings.

Recently, Duncan et al. demonstrated coding of general fluid intelligence (gF) in distributed regions, defining them as part of multi-demand (MD) systems (Assem et al., 2020; Duncan et al., 2020). The MD system encompasses a range of cognitive domains, including working memory, mathematics, language, and relational reasoning. According to Melnick et al. (2013), motion surround suppression (SI) and time thresholds for small and large gratings, which reflect hMT+ functionality, are correlated with Verbal Comprehension, Perceptual Reasoning, Working Memory, and Processing Speed indicators. Additionally, Fedorenko et al. identified multi-demand activation regions around the occipito-temporal areas, potentially overlapping with hMT+ (Fedorenko et al., 2013). As a key region in the representation of sensory flows (including optic, tactile, and auditory flows) (Fetsch et al., 2011; Gu et al., 2006), hMT+ shows potential to be central to the MD system. Future research could focus on multi-task paradigms to further investigate the mechanisms of hMT+ and its relationship with broader cognitive functions.

Together, this study offers a comprehensive insight into how the information exchange and integration between the sensory cortex (hMT+) and cognition core of BA 46, coupling with the hMT+ GABA, can predict the performance of 3D visuo-spatial ability (BDT). Our results provide direct evidence that a sensory cortex area (hMT+), its GABA biochemistry, functional connectivity, and cognition behavior levels, can assemble into complex cognition as an 3D visuo-spatial intellectual hub.

## Materials and Methods

### Subjects

Thirty-six healthy subjects (18 female, mean age: 23.6 years $\pm$ 2.1, range: 20 to 29 years) participated in this study, they were recruited from Zhejiang University. All subjects had normal or corrected-to-normal vision. In addition, they reported no psychotropic medication use, no illicit drug use within the past month, no alcohol use within 3 days prior to scanning, and right-handed. This experiment was approved by the Ethics Review Committee of Zhejiang University and conducted in accordance with the Helsinki Declaration. All participants signed informed consent forms prior to the start of the study and were compensated for their time. All subjects participated in the motion spatial suppression psychophysical, resting-state fMRI and MRS (MT+ and V1 regions, in random sequence) experiments, but only part of the MRS data (31/36 in hMT+ region and 28/36 in V1 region) survived quality control (see the part of MRS data processing). The sample size is determined by the statistic requirement (30 sample for Person correlation statistical analysis).

### Motion surrounding suppression measurement

All stimuli were generated using Matlab (MathWorks, Natick, MA) with Psychophysics Toolbox (Brainard, 1997), and were shown on a linearized monitor (1920 $\times$ 1080 resolution, 100-Hz refresh rate, Cambridge Research System, Kent, UK). The viewing distance was 72 cm from the screen, with the head stabilized by a chinrest. Stimuli were drawn against a gray (56 cd per m<sup>-2</sup>) background.

A schematic of the stimuli and trial sequences is shown in our recent study (Song et al., 2021). The stimulus was a vertical drifting sinusoidal grating (contrast, 50%; spatial frequency, 1 cycle/°; speed, 4°/s) of either small (diameter of 2°) or large (diameter of 10°) size. The edge of the grating was blurred with a raised cosine function (width, 0.3°). A cross was presented in the center of the screen at the beginning of each trial for 500ms, and participants were instructed to fixate at the cross and to keep fixating at the cross throughout the trial. In each trial, a grating of either large or

small size was randomly presented at the center of the screen. The grating drifted either leftward or rightward, and participants were asked to judge the perceived moving direction by a key press. Response time was not limited. The grating was ramped on and off with a Gaussian temporal envelope, and the grating duration was defined as 1 SD of the Gaussian function. The duration was adaptively adjusted in each trial, and duration thresholds were estimated by a staircase procedure. Thresholds for large and small gratings were obtained from a 160-trial block that contained four interleaved 3-down/1-up staircases. For each participant, we computed the correct rate for different stimulus durations separately for each stimulus size. These values were then fitted to a cumulative Gaussian function, and the duration threshold corresponding to the 75% correct point on the psychometric function was estimated for each stimulus size.

Stimulus demonstration and practice trials were presented before the first run. Auditory feedback was provided for each wrong response. To quantify the spatial suppression strength, we calculated the spatial suppression index (SI), defined as the difference of log10 thresholds for large versus small stimuli (Schallmo et al., 2018 [DOI](#); Tadin et al., 2003 [DOI](#)):

$$SI = \log_{10}(\text{large threshold}) - \log_{10}(\text{small threshold}) \quad (1)$$

## Block design task measurement

The block design task was administered in accordance with the WAIS-IV manual (Wechsler, 2008 [DOI](#)). Specifically, participants were asked to rebuild the figural pattern within a specified time limit using a set of red and white blocks. The time limits were set as 30 s to 120 s according to different levels of difficulty. The patterns were presented in ascending order of difficulty, and the test stopped if two consecutive patterns were not constructed in the allotted time. The score was determined by the accomplishment of the pattern and the time taken. A time bonus was awarded for rapid performance in the last six patterns. The score ranges between 0 and 66 points, with higher scores indicating better perceptual reasoning.

## MR experimental procedure

MR experiments were performed in a 7T whole body MR system (Siemens Healthcare, Erlangen, Germany) with a Nova Medical 32 channel array head coil. Sessions included resting-state functional MRI, fMRI localizer scan, structural image scanning, and MRS scan. Resting-state scans were acquired with 1.5-mm isotropic resolution (transverse orientation, TR/TE = 2000/20.6 ms, 160 volumes, slice number = 90, flip angle = 70°, eyes closed). Structural images were acquired using a MP2RAGE sequence (TR/ TI1/ TI2 = 5000/901/3200 ms) with 0.7-mm isotropic resolution. MRS data were collected within two regions (MT+ and V1) for each subject, and we divided them into two sessions to avoid discomfort caused by long scanning. The order of MRS VOIs (MT+ and V1) in the two sessions was counterbalanced across participants. Interval between two sessions was used for block design and motion discrimination tasks. One session included fMRI localizer scan, structural image scanning, and MRS scan for the hMT+ region; the other session included structural image scan, and MRS scan for the V1 region. Spectroscopy data were acquired using a <sup>1</sup>H-MRS single-voxel short-TE STEAM (Stimulated Echo Acquisition Mode) sequence (Frahm et al., 1989 [DOI](#)) (TE/TM/TR = 6/32/7100ms) with 4096 sampling points, 4-kHz bandwidth, 16 averages, 8 repetitions, 20×20×20 mm<sup>3</sup> VOI size, and VAPOR (variable power and optimized relaxation delays) water suppression (Tkáč et al., 1999 [DOI](#)). Prior to acquisition, first- and second-order shims were adjusted using FASTMAP (fast, automatic shimming technique by mapping along projections) (Gruetter, 1993 [DOI](#)). Two non-suppressed water spectra were also acquired: one for phase and eddy current correction (only RF pulse, 4 averages) and another for metabolite quantification (VAPOR none, 4 averages). Voxels were positioned based on anatomical landmarks using a structural image scan collected in the same session, while avoiding contamination by CSF, bone, and fat. The hMT+ VOIs were placed in the ventrolateral occipital lobe, which was based on anatomical landmarks (Dumoulin et al., 2000 [DOI](#); Schallmo et al., 2018 [DOI](#)). We did not distinguish between the middle temporal (MT) and medial superior temporal (MST) areas in these hMT+ VOIs (Huk et al.,

2002). For 14 subjects, we also functionally identified hMT+ as a check on the placement of the VOI. A protocol was used with a drifting grating (15% contrast) alternated with a static grating across blocks (10 s block duration, 160 TRs total). Using fMRI BOLD signals, these localizer data were processed online to identify the hMT+ voxels in the lateral occipital cortex, which responded more strongly to moving vs. static gratings. In addition, we only used the left hMT+ as the target region to scan, which was motivated by studies showing that left hMT+ was more effective at causing perceptual effects (Tadin et al., 2011). For V1 region, the VOI was positioned on each subject's calcarine sulcus on the left side (Tadin et al., 2011) based on anatomical landmarks (Boucard et al., 2007; Dumoulin et al., 2000).

## MRS data processing

Spectroscopy data were preprocessed and quantified using magnetic resonance signal processing and analysis, <https://www.cmrr.umn.edu/downloads/mrspa/>, which runs under MATLAB and invokes the interface of the LCModel (Version 6.3-1L) (Chen et al., 2019). First, we used the non-suppressed water spectra to perform eddy current correction and frequency/phase correction. Second, we checked the quality of each FID (16 averages) visually and removed those with obviously poor quality. Third, the absolute concentrations of each metabolite were quantitatively estimated via the Water-Scaling method. For partial-volume correction, the tissue water content was computed as follows (Ernst et al., 1993):

$$\text{Tissue water content} = f_{gm} * 0.78 + f_{wm} * 0.65 + f_{csf} * 0.97 \quad (2)$$

where  $f_{gm}$ ,  $f_{wm}$ , and  $f_{csf}$  were the GM/WM/CSF volume fraction in MRS VOI and we used FAST (fMRI's automated segmentation tool, part of the FSL toolbox) (Zhang et al., 2001) to segment the three tissue compartments from the T1-weighted structural brain images. For water T2 correction, we set water T2 as 47ms (Marjańska et al., 2012). Our concentrations were mM per kg wet weight. Furthermore, LCModel analysis was performed on all spectra within the chemical shift range of 0.2 to 4.0 ppm.

Poor spectral quality was established by a Cramer-Rao Lower Bound (CRLB) of more than 20% (Cavassila et al., 2001), and some data were excluded from further analysis. The details were described in our recently paper (Song et al., 2021).

## Rs-fMRI data processing and analysis

Resting-state functional image was analyzed in the Data Processing and Analysis for Brain Imaging DPABI toolbox (Yan et al., 2016) based on SPM 12 (<http://www.fil.ion.ucl.ac.uk/spm/>). The preprocessing steps included discard of the first five volumes, slice timing, realignment to the 90th slice, coregistration of each subject's T1-weighted anatomical and functional images, segmentation of the anatomical images into six types of tissues using DARTEL, linear detrend, regressing nuisance variables (including realignment Friston 24-parameter, global signal, white matter and CSF signal) (Friston et al., 1996), normalization to the standard Montreal Neurological Institute (MNI) space with the voxel size of  $1.5 \times 1.5 \times 1.5 \text{ mm}^3$  using DARTEL, spatial smoothing with a Gaussian kernel of 3 mm full-width-half-maximum (FWHM), and band-pass filtering with Standard frequency band (SFB, 0.01–0.1 Hz). Spherical ROI with a radius of 6mm was placed in left MT. The coordinate for left MT (-46, -72, -4, in MNI space) was obtained by our localizer fMRI experiment. We calculated the seed-to-voxel whole brain FC map for each subject. All the FC values were Fisher-Z-transformed.

We did a similar connectivity-behavior analysis to a previous study (Song et al., 2008). First, we computed the Pearson's correlation coefficient between BDT scores and the FC values across subjects in a voxel-based way. Then, to evaluate the significance, we transformed the  $r$ -value into  $t$ -value ( $t = \frac{df \cdot r}{\sqrt{1-r^2}}$ ), where  $df$  denotes to the degrees of freedom, and  $r$  is the Pearson's correlation coefficient between BDT scores and the FC values. Here,  $df$  was equal to 27. The brain regions in


which the FC values to the seed region was significantly correlated with the BDT scores were obtained with a threshold of  $P < 0.005$  for regions of *a priori* ( $|t_{(27)}| \geq 3.057$ , and adjacent cluster size  $\geq 23$  voxels (AlphaSim corrected)), and  $P < 0.01$  for whole-brain analyses ( $|t_{(27)}| \geq 2.771$  and adjacent cluster size  $\geq 37$  voxels (AlphaSim corrected)).

## Statistical Analysis

PROCESS version 3.4, a toolbox in SPSS, was used to examine the mediation model. There are some prerequisites for mediation analysis: the independent variable should be a significant predictor of the mediator, and the mediator should be a significant predictor of the dependent variable.

SPSS 20 (IBM, USA) was used to conduct all the remaining statistical analysis in the study. We evaluated the correlation of variables (GABA, Glu, SI, BDT) using Pearson's correlation analysis. Differences or correlations were considered statistically significant if  $P < 0.05$ . Significances with multiple comparisons were tested with false discovery rate (*FDR*) correction. The effect of age on intelligence was controlled for by using partial correlation in the correlation analysis and was taken as a covariate in the serial mediation model analysis.

## Data availability

Source data are provided with this paper and have been archived at GitHub and could be downloaded with reasonable request. [https://github.com/Yrehearsal/GABA\\_hMT\\_Intelligence](https://github.com/Yrehearsal/GABA_hMT_Intelligence) .

## Code availability

This paper does not report original code.

## Acknowledgements

The authors thank Prof. Dost Ongur and Fei Du for guidance on the MRS data processing, and thank Zhejiang University 7T Brain Imaging Research Center. Thank Prof. Xinyi Lai for supporting MRI data acquisition. Thank Fen Yang for technical assistance. This work was supported by STI 2030—Major Projects (2021ZD0200401 to X.M.S., 2022ZD0206000 to R.B.), the National Natural Science Foundation of China

Grants (U1909205, 61876222, 32000761, 82222032), Humanities and Social Sciences Ministry of Education (20YJC880095, 18YJA190001), the Key R&D Program of Zhejiang (2022C03096 to X.M.S., 2022ZJJH02-06 to G.C.), the European Union's Horizon 2020 Framework Program for Research and Innovation under the Specific Grant Agreement No. 785907 (Human Brain Project SGA2 to G.N.), and the MOE Frontier Science Center for Brain Science & Brain- Machine Integration, Zhejiang University.

## Author contributions

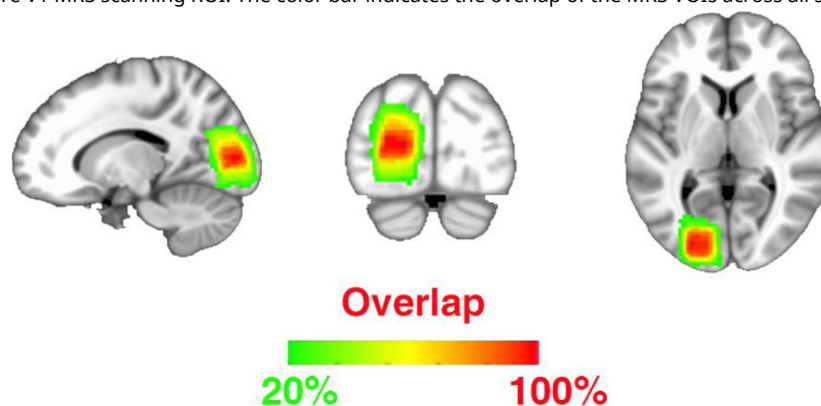
S.X.M. and Y.G. designed the experiment and G.N. guided the logic of the analysis. Y.G., Y.C. and D.L. conducted human experiments, analyzed data, and Y.G. created figures. R.B. guided the MRI experiments. J.Y., J.W. and B.X. were in charge of data collection and partial data analysis. T. W., M.L. and G.C. guided the data analysis. S.X.M., Y.G. and G.N. wrote the manuscript.

## Competing interests

The authors declare no competing interests.

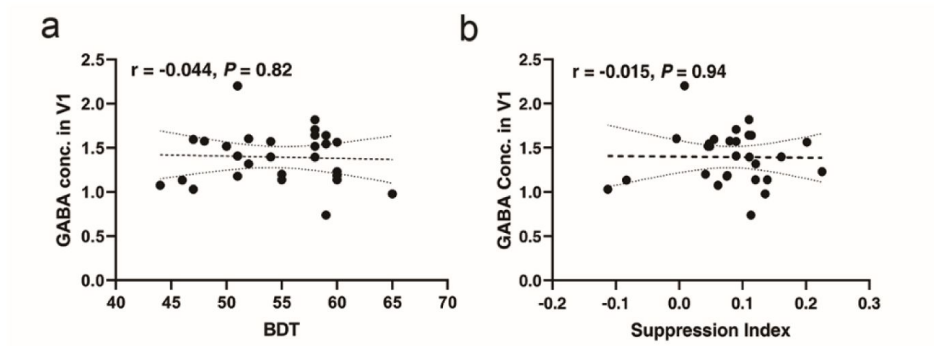
### Figure supplement 1.

The left hemisphere V1 MRS scanning ROI. The color bar indicates the overlap of the MRS VOIs across all subjects.



### Figure supplement 2.

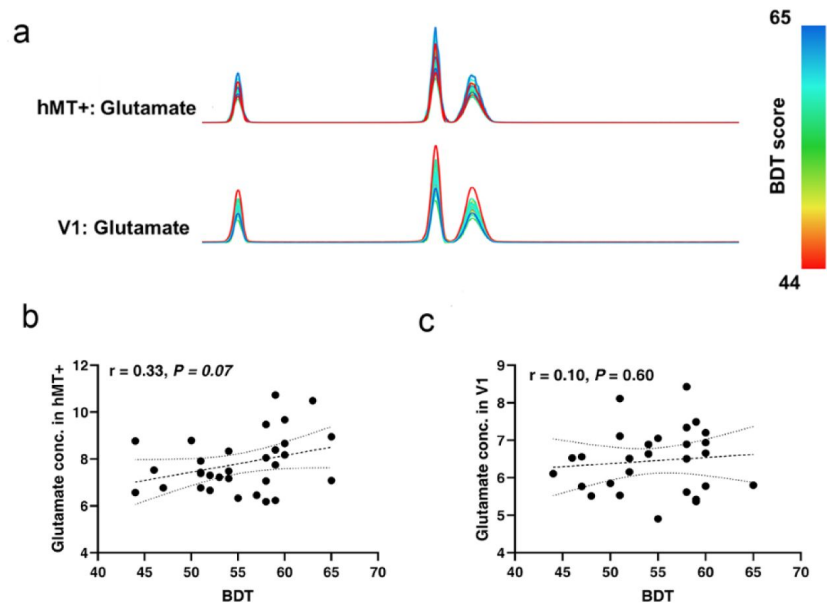
Relationships between GABA concentration in V1 and BDT/SI. **(a)** There is no significant relationship between BDT and GABA concentrations in V1. **(b)** There is also no correlation between SI and GABA concentrations in V1. GABA concentration (Conc.) is absolute, with units of mmol per kg wet weight (Methods).





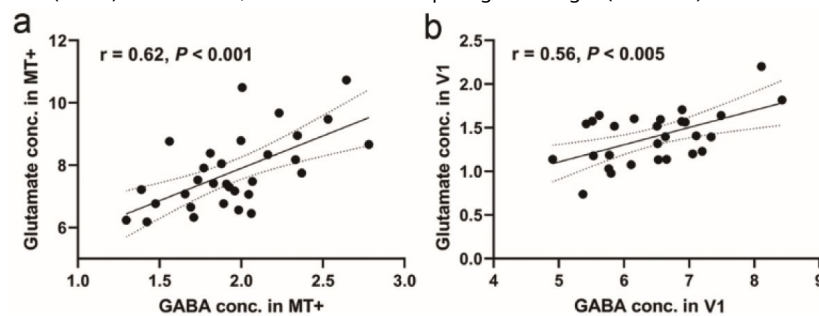
### Figure supplement 3.

Individual Glu MRS spectra from hMT+ / V1 regions and relationships between BDT and Glu concentrations in hMT+ / V1 regions. **(a)** Individual participant fitted Glutamate MRS spectra from the hMT+ (top,  $n = 31$ ) and V1 (bottom,  $n = 28$ ) voxels from baseline measurement. The colors of the Glutamate spectra represent the individual differences of BDT. The color bar represents the scores of BDT. **(b)** There is no significant relationship between BDT and Glu concentrations in hMT+. **(c)** There is also no significant correlation between BDT and Glu concentrations in V1. Glutamate concentration (Conc.) is absolute, with units of mmol per kg wet weight (Methods).



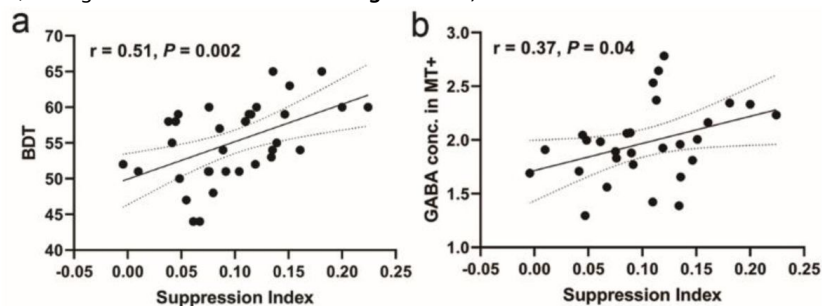
### Figure supplement 4.

Correlations between GABA and Glu concentrations in hMT+ and V1 regions. **(a)** There is significant correlation between GABA and Glu concentrations in hMT+ region. **(b)** The levels of GABA also significantly correlate with Glu in V1 region. GABA and Glu concentrations (Conc.) are absolute, with units of mmol per kg wet weight (Methods).



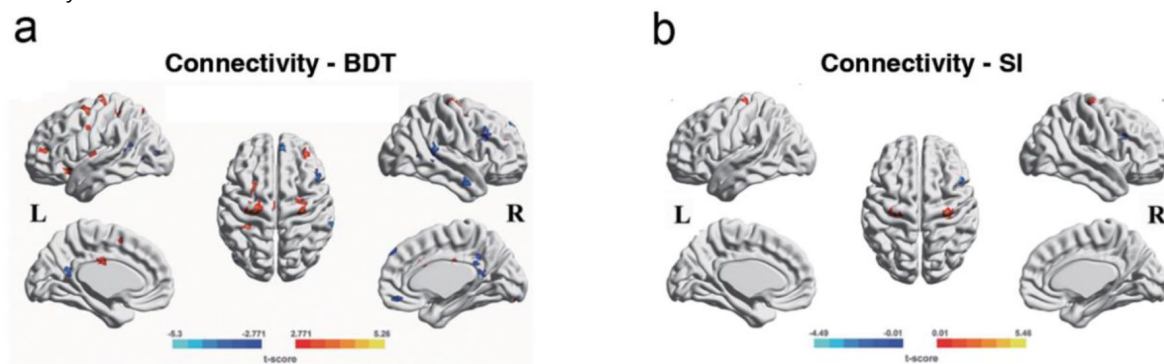
### Figure supplement 5.

Two linear correlations. **(a)** Significant positive correlation between suppression index and BDT scores (took out two outliers, having the similar result shown in **Figure 2e**). **(b)** BDT also significantly correlates with GABA concentration in hMT+ region (without two outliers, having the similar result shown in **Figure 2d**).



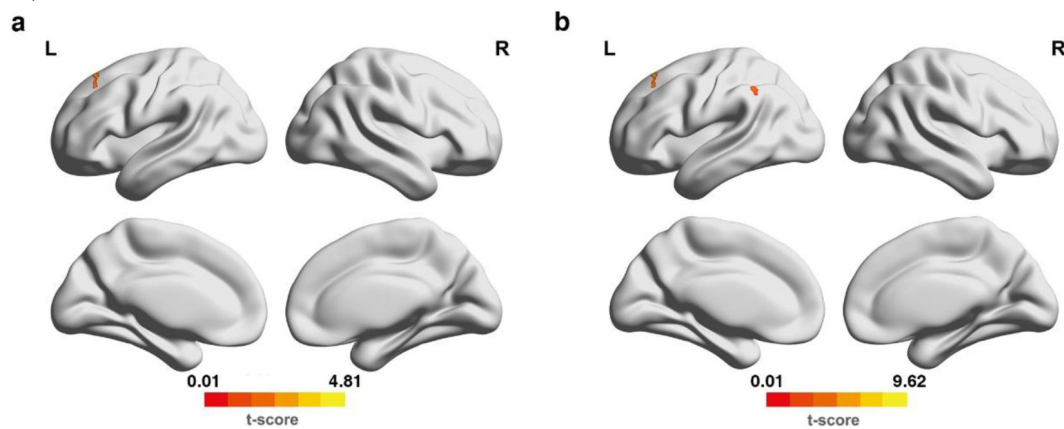
### Figure supplement 6.

Significant FCs searched from connectivity-behavior (BDT/SI) analyses in the whole brain. The seed region is the left hMT+. The significant FCs are obtained from the entire brain search, single voxel threshold  $P < 0.01$ , adjacent size  $\geq 37$  voxels (AlphaSim correcting, Methods). Positive correlations are shown in warm colors, while, negative correlations are shown in cold colors. **(a)** the significant FCs obtained from connectivity-BDT analysis. **(b)** the significant FCs obtained from connectivity-SI analysis.



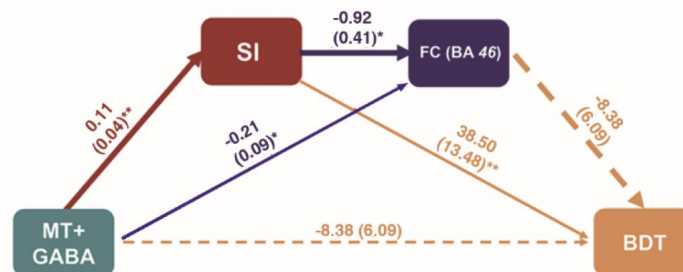
### Figure supplement 7.

Significant FCs searched from connectivity-behavior (BDT) analyses in the frontal **(a)** and whole brain **(b)**. The seed region is the left V1. **(a)** The significant FCs are obtained from the frontal search, single voxel threshold  $P < 0.005$ , adjacent size  $\geq 23$  (AlphaSim correcting, same methods for hMT+). **(b)** The significant FCs are obtained from the entire brain search, single voxel threshold  $P < 0.01$ , adjacent size  $\geq 37$  voxels (AlphaSim correcting, same methods for hMT+). Only positive correlations were detected, shown in warm colors.



### Figure supplement 8.

The alternative serial mediation models from local hMT+ GABA to global performance of BDT. The pathway that hMT+ GABA was predicted to be associated with SI, followed by the FC of hMT+ - BA 46, and then BDT, did not yield the chained mediation effects on BDT. \*:  $P < 0.05$ ; \*\*:  $P < 0.01$ ; \*\*\*:  $P < 0.001$ .



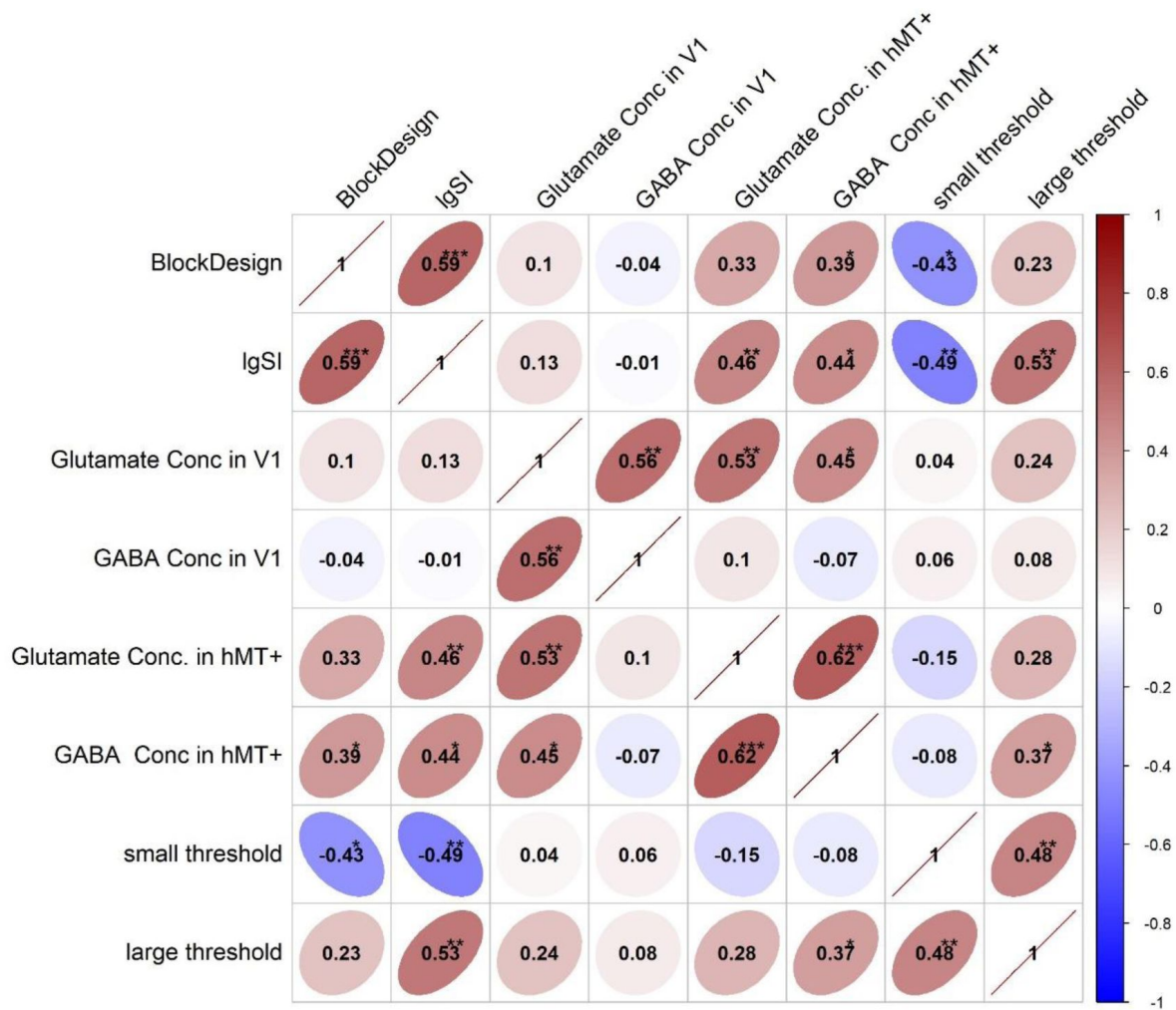


**Figure supplement 9.**

Correlation matrix shows correlations between all measured in our biochemistry and behaviour level. \*:  $P < 0.05$ , \*\*:  $P < 0.01$ , \*\*\*:  $P < 0.001$ .

FC number	Connected regions	BA	Size	Peak coordinate	<i>r</i>	<i>P</i>
				MNI (x, y, z)		
1	Frontal_Med_OrbR	11	44	(2,43.5, -12)	-0.58	0.0009
2	Frontal_Inf_Oper_R	45	49	(43.5,16.5,6)	0.64	0.0002
3	Precentral_L	6	46	(-49.5, -1.5,34.5)	0.59	0.0007
4	Precentral_L	6	237	(-24, -18,66)	0.68	0.0001
5	Precentral_R	6	80	(31, -25,72)	0.67	0.0001
6	Frontal_Mid_L	10	82	(-33,48,12)	0.62	0.0003
7	Insula_L	47	124	(-33,15, -9)	0.64	0.0002
8	Insula_L	13	107	(-31.5,9,10.5)	0.63	0.0002
9	Insula_L	13	44	(-42, -10.5,7.5)	0.64	0.0002
10	Frontal_Inf_Oper_R	44	49	(51,7.5,21)	0.59	0.0007
11	Frontal_Inf_Oper_R	46	96	(49.5,16.5,28.5)	-0.62	0.0003
12	Frontal_Mid_R	10	102	(31.5,36,30)	0.59	0.0009
13	Paracentral_Lobule_L	6	46	(-15,21,51)	-0.64	0.0002
14	Supp_Motor_Area_L	6	48	(-10.5,6,54)	0.63	0.0003
15	Frontal_Mid_L	6	119	(-24,4.5,55.5)	-0.67	0.0001
16	Frontal_Sup_R	6	136	(29, -9,65)	0.57	0.0014
17	Frontal_Sup_MedialR	9	90	(8,51,43)	-0.59	0.0009
18	Frontal_Mid_R	9	108	(50,19,41)	-0.67	0.0001
19	Occipital_Mid_L	19	47	(-43, -83,9)	-0.64	0.0002
20	Occipital_Mid_L	37	45	(-40.5, -63,4.5)	-0.62	0.0004
21	Temporal_Mid_R	39	56	(45, -57,4.5)	-0.71	0.0000
22	Temporal_Mid_L	39	54	(-45, -48,12)	-0.55	0.0021
23	Temporal_Mid_L	40	102	(-48, -55.5,16.5)	-0.65	0.0001
24	Temporal_Mid_R	21	105	(64, -2, -19)	-0.61	0.0004
25	Temporal_Sup_R	22	228	(65, -42,11)	-0.6	0.0006
26	Precuneus_L	30	155	(1.5, -51,16.5)	-0.64	0.0002
27	Cingulum_Ant_R	32	41	(9,15,27)	0.68	0.0000
28	Cingulum_Mid_R	31	73	(15, -46.5,36)	-0.63	0.0002
29	Cingulum_Mid_L	23	80	(-3, -15,30)	0.63	0.0003
30	Lingual_R	18	46	(21, -93, -16)	0.58	0.0009
31	Parietal_Sup_L	7	54	(-19.5, -63,55.5)	0.66	0.0001
32	Parietal_Sup_L	7	48	(-23, -71,58)	0.63	0.0003
33	Postcentral_L	40	41	(-31.5, -39,58.5)	0.68	0.0001
34	Postcentral_L	40	40	(-48, -36,58)	0.71	0.0000
35	Thalamus_L	Wm	108	(-24, -31.5,12)	0.64	0.0002
36	Parietal_Sup_L	5	37	(-37, -48,63)	0.59	0.0008
37	Vermis_10	-	37	(-3, -43, -37)	-0.68	0.0001
38	-	-	40	(12, -19.5, -42)	-0.68	0.0000

Single voxel threshold  $P < 0.01$  ( $t > 2.771$  or  $t < -2.771$ ), adjacent size  $\geq 37$  voxels (AlphaSim corrected).

#### Table supplement 1.

**FC of voxels showing significant correlation with BDT scores across subjects in whole brain.**

**Table supplement 2.**

**FCs of voxels showing significant correlation with SI across subjects in frontal cortex.**

FC number	Connected regions	BA	Size	Peak coordinate	<i>r</i>	<i>P</i>
				MNI ( <i>x, y, z</i> )		
1	Frontal_Inf_Oper_R	46	80	(48,15,28.5)	-0.65	0.0001
2	Precentral_R	4/6	106	(33, -25.5,63)	0.72	0.0000
3	Precentral_L	6	26	(-30, -24,72)	0.66	0.0001

Single voxel threshold  $P < 0.005$  ( $t > 3.057$  or  $t < -3.057$ ), adjacent size  $\geq 22$  voxels (AlphaSim corrected).

**Table supplement 3.**

**FCs of voxels showing significant correlation with SI across subjects in whole Brain.**

FC number	Connected regions	BA	Size	Peak coordinate	<i>r</i>	<i>P</i>
				MNI ( <i>x, y, z</i> )		
1	Cerebellum_Crus1_L	18	70	(-29, -85, -24)	0.51	0.0052
2	Cerebellum_6_R	18	39	(12, -85, -17)	0.65	0.0002
3	Calcarine_R	18	70	(15, -91.5,12)	0.63	0.0003
4	Frontal_Inf_Oper_R	46	127	(48,15,28.5)	-0.65	0.0001
5	Precentral_R	4/6	179	(32, -24,70)	0.71	0.0001
6	Precentral_L	6	59	(-30, -23,72)	0.66	0.0001
7	-	-	37	(26, -37, -11)	-0.67	0.0001

Single voxel threshold  $P < 0.01$  ( $t > 2.771$  or  $t < -2.771$ ), adjacent size  $\geq 37$  voxels (AlphaSim corrected).



FC number	hMT+ GABA concentrations			hMT+ Glu concentrations		
	<i>r</i>	<i>P</i>	<i>FDR</i>	<i>r</i>	<i>P</i>	<i>FDR</i>
1	-0.13	0.49	0.55	-0.08	0.68	0.84
2	0.17	0.38	0.49	0.05	0.82	0.88
3	0.39	0.04	0.22	0.22	0.24	0.69
4	0.41	0.03	0.19	0.24	0.21	0.69
5	<b>0.69</b>	<b>0.0001</b>	<b>0.0038**</b>	0.47	0.01	0.38
6	0.2	0.3	0.41	0.1	0.6	0.81
7	0.26	0.17	0.34	0.21	0.28	0.69
8	0.22	0.24	0.35	0.25	0.19	0.69
9	0.23	0.23	0.35	0.02	0.9	0.92
10	-0.13	0.49	0.55	-0.16	0.41	0.70
11	<b>-0.56</b>	<b>0.0018</b>	<b>0.03*</b>	-0.22	0.25	0.69
12	0.2	0.3	0.41	0.05	0.81	0.88
13	-0.35	0.06	0.25	0.07	0.73	0.84
14	0.39	0.03	0.19	0.31	0.1	0.69
15	0.006	0.98	0.98	0.14	0.46	0.70
16	0.26	0.18	0.34	0.16	0.4	0.70
17	0.15	0.42	0.51	0.04	0.83	0.88
18	-0.4	0.03	0.19	-0.21	0.27	0.69
19	-0.37	0.05	0.24	-0.15	0.44	0.70
20	-0.16	0.39	0.49	-0.19	0.33	0.70
21	-0.31	0.1	0.28	-0.29	0.13	0.69
22	-0.22	0.24	0.35	-0.07	0.72	0.84
23	-0.1	0.6	0.65	-0.12	0.53	0.77
24	-0.09	0.64	0.68	-0.09	0.63	0.83
25	-0.3	0.11	0.28	-0.14	0.46	0.70
26	-0.08	0.66	0.68	-0.08	0.69	0.84
27	0.28	0.13	0.29	0.1	0.59	0.81
28	-0.27	0.16	0.34	-0.2	0.29	0.69
29	0.33	0.08	0.28	0.25	0.19	0.69
30	0.24	0.21	0.35	0.19	0.32	0.70
31	0.24	0.22	0.35	0.36	0.05	0.69
32	0.23	0.24	0.35	0.23	0.23	0.69
33	0.44	0.02	0.19	0.18	0.35	0.70
34	0.32	0.09	0.28	0.002	0.99	0.99
35	0.32	0.09	0.28	0.31	0.1	0.69
36	0.30	0.11	0.28	0.22	0.25	0.69
37	-0.29	0.13	0.29	-0.23	0.23	0.69
38	-0.13	0.48	0.55	-0.15	0.42	0.70

Bold font indicates the significant correlations survived from multi correlation correction.

#### Table supplement 4.

#### Correlations between FC in Table supplement 1 and GABA/Glu concentrations in hMT+

**Table supplement 5.**

**Correlations between FCs in Table supplement 2 and GABA/Glu concentrations in hMT+.**

FC number	hMT+ GABA concentrations			hMT+ Glu concentrations		
	<i>r</i>	<i>P</i>	<i>FDR</i>	<i>r</i>	<i>P</i>	<i>FDR</i>
1	<b>-0.56</b>	<b>0.0017</b>	<b>0.0017**</b>	-0.21	0.27	0.27
2	<b>0.70</b>	<b>0.0001</b>	<b>0.0003***</b>	<b>0.49</b>	<b>0.007</b>	<b>0.021*</b>
3	<b>0.65</b>	<b>0.0001</b>	<b>0.0002**</b>	<b>0.40</b>	<b>0.03</b>	<b>0.045*</b>

\*:  $P_{FDR} < 0.05$ ; \*\*:  $P_{FDR} < 0.01$ ; \*\*\*:  $P_{FDR} < 0.001$ ; Bold font indicates the significant correlations survived from multi correlation correction.

**Table supplement 6.**

**Correlations between FCs in Table supplement 3 and GABA/Glu concentrations in hMT+.**

FC number	hMT+ GABA concentrations			hMT+ Glu concentrations		
	<i>r</i>	<i>P</i>	<i>FDR</i>	<i>r</i>	<i>P</i>	<i>FDR</i>
1	<b>0.37</b>	<b>0.049</b>	<b>0.049*</b>	0.32	0.09	>0.05
2	<b>0.37</b>	<b>0.049</b>	<b>0.049*</b>	0.41	0.025	>0.05
3	<b>0.48</b>	<b>0.008</b>	<b>0.01*</b>	0.21	0.28	>0.05
4	<b>-0.58</b>	<b>0.001</b>	<b>0.002**</b>	-0.22	0.26	>0.05
5	<b>0.69</b>	<b>0.0001</b>	<b>0.0007</b>	0.46	0.01	>0.05
6	<b>0.66</b>	<b>0.0001</b>	<b>0.0004***</b>	0.39	0.04	>0.05
7	<b>-0.48</b>	<b>0.0077</b>	<b>0.01*</b>	-0.35	0.067	>0.05

\*:  $P_{FDR} < 0.05$ ; \*\*:  $P_{FDR} < 0.01$ ; \*\*\*:  $P_{FDR} < 0.001$ ; Bold font indicates the significant correlations survived from multi correlation correction.

## References

1. Angelucci A., Levitt J. B., Walton E. J., Hupe J.-M., Bullier J., Lund J. S (2002) **Circuits for local and global signal integration in primary visual cortex** *Journal of Neuroscience* **22**:8633–8646
2. Assem M., Glasser M. F., Van Essen D. C., Duncan J. (2020) **A domain-general cognitive core defined in multimodally parcellated human cortex** *Cerebral Cortex* **30**:4361–4380
3. Boucard C. C., Hoogduin J. M., van der Grond J., Cornelissen F. W. (2007) **Occipital proton magnetic resonance spectroscopy (1H-MRS) reveals normal metabolite concentrations in retinal visual field defects** *PLoS One* **2**
4. Brainard D. H (1997) **The Psychophysics Toolbox** *Spat Vis* **10**:433–436
5. Carandini M., Heeger D. J (2011) **Normalization as a canonical neural computation** *Nat Rev Neurosci* **13**:51–62 <https://doi.org/10.1038/nrn3136>
6. Cattell, & Raymond, B (1963) **Theory of fluid and crystallized intelligence: A critical experiment** *Journal of Educational Psychology* **54**:1–22
7. Cavassila S., Deval S., Huegen C., Van Ormondt D., Graveron-Demilly D (2001) **Cramér–Rao bounds: an evaluation tool for quantitation** *NMR in Biomedicine: An International Journal Devoted to the Development and Application of Magnetic Resonance In Vivo* **14**:278–283
8. Chen X., Fan X., Hu Y., Zuo C., Whitfield-Gabrieli S., Holt D., Gong Q., Yang Y., Pizzagalli D. A., Du F (2019) **Regional GABA concentrations modulate inter-network resting-state functional connectivity** *Cerebral Cortex* **29**:1607–1618
9. Colom R., Jung R. E., Haier R. J (2006) **Distributed brain sites for the g-factor of intelligence** *Neuroimage* **31**:1359–1365 <https://doi.org/10.1016/j.neuroimage.2006.01.006>
10. Cumming B. G., DeAngelis G. C (2001) **The physiology of stereopsis** *Annu Rev Neurosci* **24**:203–238 <https://doi.org/10.1146/annurev.neuro.24.1.203>
11. Deary I. J., Penke L., Johnson W (2010) **The neuroscience of human intelligence differences** *Nature reviews neuroscience* **11**:201–211
12. Donner T. H., Siegel M., Fries P., Engel A. K (2009) **Buildup of choice-predictive activity in human motor cortex during perceptual decision making** *Curr Biol* **19**:1581–1585 <https://doi.org/10.1016/j.cub.2009.07.066>
13. Dumoulin S. O., Bittar R. G., Kabani N. J., Baker C. L., Le Goualher G., Bruce Pike G., Evans A. C. (2000) **A new anatomical landmark for reliable identification of human area V5/MT: a quantitative analysis of sulcal patterning** *Cereb Cortex* **10**:454–463 <https://doi.org/10.1093/cercor/10.5.454>
14. Duncan J., Assem M., Shashidhara S (2020) **Integrated Intelligence from Distributed Brain Activity** *Trends Cogn Sci* **24**:838–852 <https://doi.org/10.1016/j.tics.2020.06.012>

15. Duncan J., Seitz R. J., Kolodny J., Bor D., Herzog H., Ahmed A., Newell F. N., Emslie H (2000) **A neural basis for general intelligence** *Science* **289**:457–460 <https://doi.org/10.1126/science.289.5478.457>
16. Ende G (2015) **Proton Magnetic Resonance Spectroscopy: Relevance of Glutamate and GABA to Neuropsychology** *Neuropsychol Rev* **25**:315–325 <https://doi.org/10.1007/s11065-015-9295-8>
17. Ernst T., Kreis R., Ross B (1993) **Absolute quantitation of water and metabolites in the human brain. I. Compartments and water** *Journal of magnetic resonance, Series B* **102**:1–8
18. Everling S., Tinsley C. J., Gaffan D., Duncan J (2002) **Filtering of neural signals by focused attention in the monkey prefrontal cortex** *Nature neuroscience* **5**:671–676
19. Fangmeier T., Knauff M., Ruff C. C., Sloutsky V (2006) **fMRI evidence for a three-stage model of deductive reasoning** *Journal of cognitive neuroscience* **18**:320–334
20. Fetsch C. R., Pouget A., DeAngelis G. C., Angelaki D. E (2011) **Neural correlates of reliability-based cue weighting during multisensory integration** *Nat Neurosci* **15**:146–154 <https://doi.org/10.1038/nn.2983>
21. Frahm J. a., Bruhn H., Gyngell M., Merboldt K., Hänicke W., Sauter R. (1989) **Localized high-resolution proton NMR spectroscopy using stimulated echoes: initial applications to human brain in vivo** *Magnetic resonance in medicine* **9**:79–93
22. Friston K. J., Williams S., Howard R., Frackowiak R. S., Turner R (1996) **Movement-related effects in fMRI time-series** *Magnetic resonance in medicine* **35**:346–355
23. Gautama T., Van Hulle M. M. (2001) **Function of center-surround antagonism for motion in visual area MT/V5: a modeling study** *Vision Res* **41**:3917–3930 [https://doi.org/10.1016/s0042-6989\(01\)00246-2](https://doi.org/10.1016/s0042-6989(01)00246-2)
24. Gray J. R., Chabris C. F., Braver T. S (2003) **Neural mechanisms of general fluid intelligence** *Nat Neurosci* **6**:316–322 <https://doi.org/10.1038/nn1014>
25. Gruetter R (1993) **Automatic, localized in vivo adjustment of all first-and second-order shim coils** *Magnetic resonance in medicine* **29**:804–811
26. Gu Y., Watkins P. V., Angelaki D. E., DeAngelis G. C (2006) **Visual and nonvisual contributions to three-dimensional heading selectivity in the medial superior temporal area** *J Neurosci* **26**:73–85 <https://doi.org/10.1523/jneurosci.2356-05.2006>
27. Haier R. J., Siegel Jr B. V., Nuechterlein K. H., Hazlett E., Wu J. C., Paek J., Browning H. L., Buchsbaum M. S (1988) **Cortical glucose metabolic rate correlates of abstract reasoning and attention studied with positron emission tomography** *Intelligence* **12**:199–217
28. Hayes A. F (2013) **Introduction to Mediation, Moderation, and Conditional Process Analysis: A Regression-Based Approach**
29. Huk A. C., Dougherty R. F., Heeger D. J (2002) **Retinotopy and functional subdivision of human areas MT and MST** *Journal of Neuroscience* **22**:7195–7205

30. Jung R. E., Haier R. J (2007) **The Parieto-Frontal Integration Theory (P-FIT) of intelligence: converging neuroimaging evidence** *Behav Brain Sci* **30**:135–154 <https://doi.org/10.1017/S0140525X07001185>
31. Keller A. J., Roth M. M., Scanziani M (2020) **Feedback generates a second receptive field in neurons of the visual cortex** *Nature* **582**:545–549
32. Li M., Song X. M., Xu T., Hu D., Roe A. W., Li C.-Y (2019) **Subdomains within orientation columns of primary visual cortex** *Science advances* **5**
33. Liu D. Y., Ju X., Gao Y., Han J. F., Li Z., Hu X. W., Tan Z. L., Northoff G., Song X. M (2022) **From Molecular to Behavior: Higher Order Occipital Cortex in Major Depressive Disorder** *Cereb Cortex* **32**:2129–2139 <https://doi.org/10.1093/cercor/bhab343>
34. Liu L. D., Haefner R. M., Pack C. C (2016) **A neural basis for the spatial suppression of visual motion perception** *Elife* **5**
35. Marjańska M., Auerbach E. J., Valabrègue R., Van de Moortele P. F., Adriany G., Garwood M. (2012) **Localized <sup>1</sup>H NMR spectroscopy in different regions of human brain in vivo at 7 T: T2 relaxation times and concentrations of cerebral metabolites** *NMR in Biomedicine* **25**:332–339
36. Melnick M. D., Harrison B. R., Park S., Bennetto L., Tadin D (2013) **A strong interactive link between sensory discriminations and intelligence** *Curr Biol* **23**:1013–1017 <https://doi.org/10.1016/j.cub.2013.04.053>
37. Ozeki H., Finn I. M., Schaffer E. S., Miller K. D., Ferster D (2009) **Inhibitory stabilization of the cortical network underlies visual surround suppression** *Neuron* **62**:578–592
38. Reynolds J. H., Heeger D. J (2009) **The normalization model of attention** *Neuron* **61**:168–185
39. Sato T. K., Haider B., Häusser M., Carandini M (2016) **An excitatory basis for divisive normalization in visual cortex** *Nature neuroscience* **19**:568–570
40. Schallmo M. P., Kale A. M., Millin R., Flevaris A. V., Brkanac Z., Edden R. A., Bernier R. A., Murray S. O (2018) **Suppression and facilitation of human neural responses** *Elife* **7** <https://doi.org/10.7554/eLife.30334>
41. Siegel M., Buschman T. J., Miller E. K (2015) **Cortical information flow during flexible sensorimotor decisions** *Science* **348**:1352–1355 <https://doi.org/10.1126/science.aab0551>
42. Song M., Zhou Y., Li J., Liu Y., Tian L., Yu C., Jiang T (2008) **Brain spontaneous functional connectivity and intelligence** *Neuroimage* **41**:1168–1176 <https://doi.org/10.1016/j.neuroimage.2008.02.036>
43. Song X. M. *et al.* (2021) **Reduction of higher-order occipital GABA and impaired visual perception in acute major depressive disorder** *Mol Psychiatry* **26**:6747–6755 <https://doi.org/10.1038/s41380-021-01090-5>
44. Spearman C (1904) **General Intelligence” Objectively Determined and Measured** *American Journal of Psychology* **15**:201–293
45. Tadin D (2015) **Suppressive mechanisms in visual motion processing: From perception to intelligence** *Vision Res* **115**:58–70 <https://doi.org/10.1016/j.visres.2015.08.005>

46. Tadin D., Lappin J. S., Gilroy L. A., Blake R (2003) **Perceptual consequences of centre-surround antagonism in visual motion processing** *Nature* **424**:312–315 <https://doi.org/10.1038/nature01800>
47. Tadin D., Silvanto J., Pascual-Leone A., Battelli L (2011) **Improved motion perception and impaired spatial suppression following disruption of cortical area MT/V5** *Journal of Neuroscience* **31**:1279–1283
48. Tkáč I., Starčuk Z., Choi I. Y., Gruetter R (1999) **In vivo 1H NMR spectroscopy of rat brain at 1 ms echo time** *Magnetic Resonance in Medicine: An Official Journal of the International Society for Magnetic Resonance in Medicine* **41**:649–656
49. Treue S., Maunsell J. H (1996) **Attentional modulation of visual motion processing in cortical areas MT and MST** *Nature* **382**:539–541
50. Wang X. J (2002) **Probabilistic decision making by slow reverberation in cortical circuits** *Neuron* **36**:955–968 [https://doi.org/10.1016/s0896-6273\(02\)01092-9](https://doi.org/10.1016/s0896-6273(02)01092-9)
51. Wechsler D. (2008) **Wechsler, D. (2008). Wechsler Memory Scale–Fourth Edition (WMS-IV) technical and interpretive manual.**
52. Wilming N., Murphy P. R., Meyniel F., Donner T. H (2020) **Large-scale dynamics of perceptual decision information across human cortex** *Nat Commun* **11** <https://doi.org/10.1038/s41467-020-18826-6>
53. Wimmer K., Compte A., Roxin A., Peixoto D., Renart A., de la Rocha J. (2015) **Sensory integration dynamics in a hierarchical network explains choice probabilities in cortical area MT** *Nat Commun* **6** <https://doi.org/10.1038/ncomms7177>
54. Yan C.-G., Wang X.-D., Zuo X.-N., Zang Y.-F (2016) **DPABI: data processing & analysis for (resting-state) brain imaging** *Neuroinformatics* **14**:339–351
55. Zaksas D., Pasternak T (2006) **Directional signals in the prefrontal cortex and in area MT during a working memory for visual motion task** *J Neurosci* **26**:11726–11742 <https://doi.org/10.1523/JNEUROSCI.3420-06.2006>
56. Zhang S., Xu M., Kamigaki T., Hoang Do J. P., Chang W.-C., Jenvay S., Miyamichi K., Luo L., Dan Y (2014) **Long-range and local circuits for top-down modulation of visual cortex processing** *Science* **345**:660–665
57. Zhang Y., Brady M., Smith S (2001) **Segmentation of brain MR images through a hidden Markov random field model and the expectation-maximization algorithm** *IEEE transactions on medical imaging* **20**:45–57

## Editors

Reviewing Editor

**Xilin Zhang**

South China Normal University, Guangzhou, China



Senior Editor

**Yanchao Bi**

Beijing Normal University, Beijing, China

**Reviewer #1 (Public Review):**

**Summary:**

The study of human intelligence has been the focus of cognitive neuroscience research, and finding some objective behavioral or neural indicators of intelligence has been an ongoing problem for scientists for many years. Melnick et al, 2013 found for the first time that the phenomenon of spatial suppression in motion perception predicts an individual's IQ score. This is because IQ is likely associated with the ability to suppress irrelevant information. In this study, a high-resolution MRS approach was used to test this theory. In this paper, the phenomenon of spatial suppression in motion perception was found to be correlated with the visuo-spatial subtest of gF, while both variables were also correlated with the GABA concentration of MT+ in the human brain. In addition, there was no significant relationship with the excitatory transmitter Glu. At the same time, SI was also associated with MT+ and several frontal cortex FCs.

**Strengths:**

- (1) 7T high-resolution MRS is used.
- (2) This study combines the behavioral tests, MRS, and fMRI.

**Weaknesses:**

**Major:**

- (1) In Melnick (2013) IQ scores were measured by the full set of WAIS-III, including all subtests. However, this study only used visual spatial domain of gF. I wonder why only the visuo-spatial subtest was used not the full WAIS-III? I am wondering whether other subtests were conducted and, if so, please include the results as well to have comprehensive comparisons with Melnick (2013).

**Minor:**

- (1) Table 1 and Table supplementary 1-3 contain many correlation results. But what are the main points of these values? Which values do the authors want to highlight? Why are only p-values shown with significance symbols in Table supplementary 2??
- (2) Line 27, it is unclear to me what is "the canonical theory".
- (3) Throughout the paper, the authors use "MT+", I would suggest using "hMT+" to indicate the human MT complex, and to be consistent with the human fMRI literature.
- (4) At the beginning of the results section, I suggest including the total number of subjects. It is confusing what "31/36 in MT+, and 28/36 in V1" means.
- (5) Line 138, "This finding supports the hypothesis that motion perception is associated with neural activity in MT+ area". This sentence is strange because it is a well established finding in numerous human fMRI papers. I think the authors should be more specific about what this finding implies.
- (6) There are no unit labels for all x- and y-axes in Figure 1. I only see the unit for Conc is mmol per kg wet weight.

- (7) Although the correlations are not significant in Figure supplement 2&3, please also include the correlation line, 95% confidence interval, and report the  $r$  values and  $p$  values (i.e., similar format as in Figure 1C).
- (8) There is no need to separate different correlation figures into Figure supplementary 1-4. They can be combined into the same figure.
- (9) Line 213, as far as I know, the study (Melnick et al., 2013) is a psychophysical study and did not provide evidence that the spatial suppression effect is associated with MT+.
- (10) At the beginning of the results, I suggest providing more details about the motion discrimination tasks and the measurement of the BDT.
- (11) Please include the absolute duration thresholds of the small and large sizes of all subjects in Figure 1.
- (12) Figure 5 is too small. The items in plot a and b can be barely visible.

<https://doi.org/10.7554/eLife.97545.2.sa2>

### Reviewer #3 (Public Review):

- (1) Throughout the manuscript, hMT+ connectivity with the frontal cortex has been treated as an a priori hypothesis/space. However, there is no such motivation or background literature mentioned in the Introduction. Can the authors clarify the necessity of functional connectivity? In other words, can BOLD activity of hMT+ in the localizer task substitute for functional connectivity between hMT+ and the frontal cortex?
- (2) There is an obvious mismatch between the in-text description and the content of the figure:
- "In contrast, there was no correlation between BDT and GABA levels in V1 voxels (figure supplement 1a). Further, we show that SI significantly correlates with GABA levels in hMT+ voxels ( $r = 0.44$ ,  $P = 0.01$ ,  $n = 31$ , Figure 3d). In contrast, no significant correlation between SI and GABA concentrations in V1 voxels was observed (figure supplement 1b)."
- (3) The authors' response to my previous round of review indicated that the "V1 ROIs" covered a substantial amount of V3 (32%). Therefore, it would no longer be appropriate to call these "V1 ROIs". I'd suggest renaming them as "Early Visual Cortex (EVC) ROIs" to be more accurate. Can the authors justify why choosing the left hemisphere for visual intelligence task, which is typically believed to be right lateralized?
- (4) "Small threshold" and "large threshold" are neither standard descriptions, and it is unclear what "small threshold" refers to in the following figure caption. Additionally, the unit (ms) is confusing. Does it refer to timing?
- "(f) Pearson's correlation showing significant negative correlations between BDT and small threshold."
- (5) In the response letter, the authors mentioned incorporating the neural efficiency hypothesis in the Introduction, but the revised Introduction does not contain such information.

<https://doi.org/10.7554/eLife.97545.2.sa1>

Author response:

The following is the authors' response to the original reviews.

**Public Reviews:**

**Reviewer #1 (Public Review):**

*Summary:*

*The study of human intelligence has been the focus of cognitive neuroscience research, and finding some objective behavioral or neural indicators of intelligence has been an ongoing problem for scientists for many years. Melnick et al, 2013 found for the first time that the phenomenon of spatial suppression in motion perception predicts an individual's IQ score. This is because IQ is likely associated with the ability to suppress irrelevant information. In this study, a high-resolution MRS approach was used to test this theory. In this paper, the phenomenon of spatial suppression in motion perception was found to be correlated with the visuo-spatial subtest of gF, while both variables were also correlated with the GABA concentration of MT+ in the human brain. In addition, there was no significant relationship with the excitatory transmitter Glu. At the same time, SI was also associated with MT+ and several frontal cortex FCs.*

*Strengths:*

*(1) 7T high-resolution MRS is used.*

*(2) This study combines the behavioral tests, MRS, and fMRI.*

*Weaknesses:*

*(1) In the intro, it seems to me that the multiple-demand (MD) regions are the key in this study. However, I didn't see any results associated with the MD regions. Did I miss something?*

Thank you to the reviewer for pointing this out. After careful consideration, we agree with your point of view. According to the results of Melnick 2013, the motion surround suppression (SI) and the time thresholds of small and large gratings representing hMT+ functionality are correlated with Verbal Comprehension, Perceptual Reasoning, Working Memory, and Processing Speed Indicators, with correlation coefficients of 0.69, 0.47, 0.49, and 0.50, respectively. This suggests that hMT+ does have the potential to become the core of MD system. However, due to our results only delving into “the GABA-ergic inhibition in human MT predicts visuo-spatial intelligence mediated through the frontal cortex”, it is not yet sufficient to prove that hMT+ is the core node of the MD system, we have adjusted the explanatory logic of the article. Briefly, we emphasize the de-redundancy of hMT+ in visual-spatial intelligence and the improvement of information processing efficiency, while weaken the significance of hMT+ in MD systems.

*(2) How was the sample size determined? Is it sufficient?*

Thank you to reviewer for pointing this out. We use G\*power to determine our sample size. In the study by Melnick (2013), they reported a medium effect between SI and Perception Reasoning sub-ability ( $r=0.47$ ). Here we use this  $r$  value as the correlation coefficient ( $\rho$  H1), setting the power at the commonly used threshold of 0.8 and the alpha error probability at 0.05. The required sample size is calculated to be 26. This ensures that our study has reasonable power to yield valid statistical results. Furthermore, compared to earlier within-

subject studies like Schallmo et al.'s 2018 research, which used 22 datasets to examine GABA levels in MT+ and the early visual cortex (EVC), our study includes an enough dataset.

*(3) In Schallmo elife 2018, there was no correlation between GABA concentration and SI. How can we justify the different results different here?*

Thank reviewer for pointing this out. There are several differences between us:

- a. While the earlier study by Schallmo et al. (2018) employed 3T MRS, we utilize 7T MRS, enhancing our ability to detect and measure GABA with greater accuracy.
- b. Schallmo elife 2018 choose to use the bilateral hMT+ as the MRS measurement region while we use the left hMT+. The reason why we focus on left hMT+ are describe in reviewer 1. (6). Briefly, use of left MT/V5 as a target was motivated by studies demonstrating that left MT/V5 TMS is more effective at causing perceptual effects (Tadin et al., 2011).
- c. The resolution of MRS sequence in Schallmo elife 2018 is 3 cm isotropic voxel, while we apply 2 cm isotropic voxel. This helps us more precisely locate hMT+ and exclude more white matter signal.

*(4) Basically this study contains the data of SI, BDT, GABA in MT+ and V1, Glu in MT+ and V1-all 6 measurements. There should be  $6 \times 5 / 2 = 15$  pairwise correlations. However, not all of these results are included in Figure 1 and supplementary 1-3. I understand that it is not necessary to include all figures. But I suggest reporting all values in one Table.*

We thank the reviewer for the good suggestion, we have made a correlation matrix to reporting all values in Figure Supplementary 9.

*(5) In Melnick (2013), the IQ scores were measured by the full set of WAIS-III, including all subtests. However, this study only used the visual spatial domain of gF. I wonder why only the visuo-spatial subtest was used not the full WAIS-III?*

We thank the reviewer for pointing this out. The decision was informed by Melnick's findings which indicated high correlations between Surround suppression (SI) and the Verbal Comprehension, Perceptual Reasoning, Working Memory, and Processing Speed Indexes, with correlation coefficients of 0.69, 0.47, 0.49, and 0.50, respectively. It is well-established that the hMT+ region of the brain is a sensory cortex involved in visual perception processing (3D perception). Furthermore, motion surround suppression (SI), a specific function of hMT+, aligns closely with this region's activities. Given this context, the Perception Reasoning sub-ability was deemed to have the clearest mechanism for further exploration. Consequently, we selected the most representative subtest of Perception Reasoning—the Block Design Test—which primarily assesses 3D visual intelligence.

*(6) In the functional connectivity part, there is no explanation as to why only the left MT+ was set to the seed region. What is the problem with the right MT+?*

We thank the reviewer for pointing this out. The main reason is that our MRS ROI is the left hMT+, we would like to make different models' ROI consistent to each other. Use of left MT/V5 as a target was motivated by studies demonstrating that left MT/V5 TMS is more effective at causing perceptual effects (Tadin et al., 2011).

*(7) In Melnick (2013), the authors also reported the correlation between IQ and absolute duration thresholds of small and large stimuli. Please include these analyses as well.*

We thank the reviewer for the good advice. Containing such result do help researchers compare the result between Melnick and us. We have made such figures in the revised version (Figure 3f, g).

**Reviewer #2 (Public Review):**

*Summary:*

*Recent studies have identified specific regions within the occipito-temporal cortex as part of a broader fronto-parietal, domain-general, or "multiple-demand" (MD) network that mediates fluid intelligence (gF). According to the abstract, the authors aim to explore the mechanistic roles of these occipito-temporal regions by examining GABA/glutamate concentrations. However, the introduction presents a different rationale: investigating whether area MT+ specifically, could be a core component of the MD network.*

*Strengths:*

*The authors provide evidence that GABA concentrations in MT+ and its functional connectivity with frontal areas significantly correlate with visuo-spatial intelligence performance. Additionally, serial mediation analysis suggests that inhibitory mechanisms in MT+ contribute to individual differences in a specific subset of the Wechsler Adult Intelligence Scale, which assesses visuo-spatial aspects of gF.*

*Weaknesses:*

*(1) While the findings are compelling and the analyses robust, the study's rationale and interpretations need strengthening. For instance, Assem et al. (2020) have previously defined the core and extended MD networks, identifying the occipito-temporal regions as TE1m and TE1p, which are located more rostrally than MT+. Area MT+ might overlap with brain regions identified previously in Fedorenko et al., 2013, however the authors attribute these activations to attentional enhancement of visual representations in the more difficult conditions of their tasks. For the aforementioned reasons, It is unclear why the authors chose MT+ as their focus. A stronger rationale for this selection is necessary and how it fits with the core/extended MD networks.*

We really appreciate reviewer's opinions. The reason why we focus on hMT+ is following: According to the results of Melnick 2013, the motion surround suppression (SI) and the time thresholds of small and large gratings representing hMT+ functionality are correlated with Verbal Comprehension, Perceptual Reasoning, Working Memory, and Processing Speed Indicators, with high correlation coefficients of 0.69, 0.47, 0.49, and 0.50, respectively. In addition, Fedorenko et al. 2013, the averaged MD activity region appears to overlap with hMT+. Based on these findings, we assume that hMT+ does have the potential to become the core of MD system.

*(2) Moreover, although the study links MT+ inhibitory mechanisms to a visuo-spatial component of gF, this evidence alone may not suffice to position MT+ as a new core of the MD network. The MD network's definition typically encompasses a range of cognitive domains, including working memory, mathematics, language, and relational reasoning. Therefore, the claim that MT+ represents a new core of MD needs to be supported by more comprehensive evidence.*

Thank reviewer for pointing this out. After careful consideration, we agree with your point of view. Due to our results only delving into visuo-spatial intelligence, it is not yet sufficient to prove that hMT is the core node of the MD system. We will adjust the explanatory logic of the article, that is, emphasizing the de-redundancy of hMT+in visual-spatial intelligence and the

improvement of information processing efficiency, while weakening the significance of hMT+ in MD systems.

**Reviewer #3 (Public Review):**

*Summary:*

*This manuscript aims to understand the role of GABA-ergic inhibition in the human MT+ region in predicting visuo-spatial intelligence through a combination of behavioral measures, fMRI (for functional connectivity measurement), and MRS (for GABA/glutamate concentration measurement). While this is a commendable goal, it becomes apparent that the authors lack fundamental understanding of vision, intelligence, or the relevant literature. As a result, the execution of the research is less coherent, dampening the enthusiasm of the review.*

*Strengths:*

*(1) Comprehensive Approach: The study adopts a multi-level approach, i.e., neurochemical analysis of GABA levels, functional connectivity, and behavioral measures to provide a holistic understanding of the relationship between GABA-ergic inhibition and visuo-spatial intelligence.*

*(2) Sophisticated Techniques: The use of ultra-high field magnetic resonance spectroscopy (MRS) technology for measuring GABA and glutamate concentrations in the MT+ region is a recent development.*

*Weaknesses:*

*Study Design and Hypothesis*

*(1) The central hypothesis of the manuscript posits that "3D visuo-spatial intelligence (the performance of BDT) might be predicted by the inhibitory and/or excitation mechanisms in MT+ and the integrative functions connecting MT+ with the frontal cortex." However, several issues arise:*

*(1.1) The Suppression Index depicted in Figure 1a, labeled as the "behavior circle," appears irrelevant to the central hypothesis.*

We thank the reviewer for pointing this out. In our study, the inhibitory mechanisms in hMT+ are conceptualized through two models: the neurotransmitter model and the behavioral model. The Suppression Index is essential for elucidating the local inhibitory mechanisms within the behavioral model. However, we acknowledge that our initial presentation in the introduction may not have clearly articulated our hypothesis, potentially leading to misunderstandings. We have revised the introduction to better clarify these connections and ensure the relevance of the Suppression Index is comprehensively understood.

*(1.2) The construct of 3D visuo-spatial intelligence, operationalized as the performance in the Block Design task, is inconsistently treated as another behavioral task throughout the manuscript, leading to confusion.*

We thank the reviewer for pointing this out. We acknowledge that our manuscript may have inconsistently presented this construct across different sections, causing confusion. To address this, we ensured a consistent description of 3D visuo-spatial intelligence in both the introduction and the discussion sections. But we maintained 'Block Design task score' within the results section to help readers clarify which subtest we use.



*(1.3) The schematics in Figure 1a and Figure 6 appear too high-level to be falsifiable. It is suggested that the authors formulate specific and testable hypotheses and preregister them before data collection.*

We thank the reviewer for pointing this out. We have revised the Figure 1a and made it less abstract and more logical. For Figure 6, the schematic represents our theoretical framework of how hMT+ contributes to 3D visuo-spatial intelligence, we believe the elements within this framework are grounded in related theories and supported by evidence discussed in our results and discussions section, making them specific and testable.

*(2) Central to the hypothesis and design of the manuscript is a misinterpretation of a prior study by Melnick et al. (2013). While the original study identified a strong correlation between WAIS (IQ) and the Suppression Index (SI), the current manuscript erroneously asserts a specific relationship between the block design test (from WAIS) and SI. It should be noted that in the original paper, WAIS comprises Similarities, Vocabulary, Block design, and Matrix reasoning tests in Study 1, while the complete WAIS is used in Study 2. Did the authors conduct other WAIS subtests other than the block design task?*

Thank you for pointing this out. Reviewer #1 also asked this question, we copy the answers in here “The decision was informed by Melnick’s findings which indicated high correlations between Surround suppression (SI) and the Verbal Comprehension, Perceptual Reasoning, Working Memory, and Processing Speed Indexes, with correlation coefficients of 0.69, 0.47, 0.49, and 0.50, respectively. It is well-established that the hMT+ region of the brain is a sensory cortex involved in visual perception processing (3D perception). Furthermore, motion surround suppression (SI), a specific function of hMT+, aligns closely with this region’s activities. Given this context, the Perception Reasoning sub-ability was deemed to have the clearest mechanism for further exploration. Consequently, we selected the most representative subtest of Perception Reasoning—the Block Design Test—which primarily assesses 3D visual intelligence.”

*(3) Additionally, there are numerous misleading references and unsubstantiated claims throughout the manuscript. As an example of misleading reference, “the human MT ... a key region in the multiple representations of sensory flows (including optic, tactile, and auditory flows) (Bedny et al., 2010; Ricciardi et al., 2007); this ideally suits it to be a new MD core.” The two references in this sentence are claims about plasticity in the congenitally blind with sensory deprivation from birth, which is not really relevant to the proposal that hMT+ is a new MD core in healthy volunteers.*

Thank you for pointing this out. We have carefully read the corresponding references and considered the corresponding theories and agree with these comments. Due to our results only delving into “the GABA-ergic inhibition in human MT predicts visuo-spatial intelligence mediated by reverberation with frontal cortex”, it is not yet sufficient to prove that hMT+ is the core node of the MD system, we will adjust the explanatory logic of the article, that is, emphasizing the de redundancy of hMT+ in visual-spatial intelligence and the improvement of information processing efficiency, while weakening the significance of hMT+ in MD systems. In addition, regarding the potential central role of hMT+ in the MD system, we agree with your view that research on hMT+ as a multisensory integration hub mainly focuses on developmental processes. Meanwhile, in adults, the MST region of hMT+ is considered a multisensory integration area for visual and vestibular inputs, which potentially supports the role of hMT+ in multitasking multisensory systems (Gu et al., J. Neurosci, 26(1), 73–85, 2006; Fetsch et al., Nat. Neurosci, 15, 146–154, 2012.). Further research could explore how other intelligence sub-ability such as working memory and language comprehension are facilitated by hMT+'s features.



*Another example of unsubstantiated claim: the rationale for selecting V1 as the control region is based on the assertion that "it mediates the 2D rather than 3D visual domain (Born & Bradley, 2005)". That's not the point made in the Born & Bradley (2005) paper on MT. It's crucial to note that V1 is where the initial binocular convergence occurs in cortex, i.e., inputs from both the right and left eyes to generate a perception of depth.*

Thank you for pointing this out. We acknowledge the inappropriate citation of "Born & Bradley, 2005," which focuses solely on the structure and function of the visual area MT. However, we believe that choosing hMT+ as the domain for 3D visual analysis and V1 as the control region is justified. Cumming and DeAngelis (Annu Rev Neurosci, 24:203–238.2001) state that binocular disparity provides the visual system with information about the three-dimensional layout of the environment, and the link between perception and neuronal activity is stronger in the extrastriate cortex (especially MT) than in the primary visual cortex. This supports our choice and emphasizes the relevance of hMT+ in our study. We have revised our reference in the revised version.

#### *Results & Discussion*

*(1) The missing correlation between SI and BDT is crucial to the rest of the analysis. The authors should discuss whether they replicated the pattern of results from Melnick et al. (2013) despite using only one WAIS subtest.*

We thank for the reviewer's suggestion. We have placed it in the main text (Figure 3e).

*(2) ROIs: can the authors clarify if the results are based on bilateral MT+/V1 or just those in the left hemisphere? Can the authors plot the MRS scan area in V1? I would be surprised if it's precise to V1 and doesn't spread to V2/3 (which is fine to report as early visual cortex).*

We thank for the reviewer's suggestion. We have drawn the V1 ROI MRS scanning area (Figure supplement 1). Using the template, we checked the coverage of V1, V2, and V3. Although the MRS overlap regions extend to V2 (3%) and V3 (32%), the major coverage of the MRS scanning area is in V1, with 65% overlap across subjects.

*(3) Did the authors examine V1 FC with either the frontal regions and/or whole brain, as a control analysis? If not, can the author justify why V1 serves as the control region only in the MRS but not in FC (Figure 4) or the mediation analysis (Figure 5)? That seems a little odd given that control analyses are needed to establish the specificity of the claim to MT+.*

We thank for the reviewer's suggestion. We have done the V1 FC-behavior connection as control analysis (Figure supplement 7). Only positive correlations in the frontal area were detected, suggesting that in the 3D visuo-spatial intelligence task, V1 plays a role in feedforward information processing. However, hMT+, which showed specific negative correlations in the frontal, is involved in the inhibition mechanism. These results further emphasize the de-redundancy function of hMT+ in 3D visuo-spatial intelligence.

Regarding the mediation analysis, since GABA/Glu concentration in V1 has no correlation with BDT score, it is not sufficient to apply mediation analysis.

*(4) It is not clear how to interpret the similarity or difference between panels a and b in Figure 4.*

We thank the reviewer for pointing this out. We have further interpreted the difference between a and b in the revised version. Panels a represents BDT score correlated hMT+-region FC, which is obviously involved in frontal cortex. While panels b represents SI correlated hMT+-region FC, which shows relatively less regions. The overlap region is what we are interested in and explain how local inhibitory mechanisms works in the 3D visuo-spatial intelligence. In addition, we have revised Figure 4 and point out the overlap region.

*(5) SI is not relevant to the authors' priori hypothesis, but is included in several mediation analyses. Can the authors do model comparisons between the ones in Figure 5c, d, and Figure S6? In other words, is SI necessary in the mediation model? There seem discrepancies between the necessity of SI in Figures 5c/S6 vs. Figure 5d.*

We thank the reviewer for highlighting this point. The relationship between the Suppression Index (SI) and our a priori hypotheses is elaborated in the response to reviewer 3, section (1). SI plays a crucial role in explicating how local inhibitory mechanisms, on the psychological level, function within the context of the 3D visuo-spatial task. Additionally, Figure 5c illustrates the interaction between the frontal cortex and hMT+, showing how the effects from the frontal cortex (BA46) on the Block Design Task are fully mediated by SI. This further underscores the significance of SI in our model.

*(6) The sudden appearance of "efficient information" in Figure 6, referring to the neural efficiency hypothesis, raises concerns. Efficient visual information processing occurs throughout the visual cortex, starting from V1. Thus, it appears somewhat selective to apply the neural efficiency hypothesis to MT+ in this context.*

We thank the reviewer for highlighting this point. There is no doubt that V1 involved in efficient visual information processing. However, in our result, the V1 GABA has no significant correlation between BDT score, suggesting that the V1 efficient processing might not sufficiently account for the individual differences in 3D visuo-spatial intelligence. Additionally, we will clarify our use of the neural efficiency hypothesis by incorporating it into the introduction of our paper to better frame our argument.

#### *Transparency Issues:*

*(1) Don't think it's acceptable to make the claim that "All data needed to evaluate the conclusions in the paper are present in the paper and/or the Supplementary information". It is the results or visualizations of data analysis, rather than the raw data themselves, that are presented in the paper/supp info.*

We thank the reviewer for pointing this out. We realized that such expression would lead to confusion. We have deleted this expression.

*(2) No GitHub link has been provided in the manuscript to access the source data, which limits the reproducibility and transparency of the study.*

We thank the reviewer for pointing this out. We have attached the GitHub link in the revised version.

#### *Minor:*

*"Locates" should be replaced with "located" throughout the paper. For example: "To investigate this issue, this study selects the human MT complex (hMT+), a region located at the occipito-temporal border, which represents multiple sensory flows, as the target brain area."*

We thank the reviewer for pointing this out. We have revised it.

| *Use "hMT+" instead of "MT+" to be consistent with the term in the literature.*

We thank the reviewer for pointing this out. We agree to use hMT+ in the literature.

| *"Green circle" in Figure 1 should be corrected to match its actual color.*

We thank the reviewer for pointing this out. We have revised it.

| *The abbreviation for the Wechsler Adult Intelligence Scale should be "WAIS," not "WASI."*

We thank the reviewer for pointing this out. We have revised it.

**Recommendations for the authors:**

**Reviewer #1 (Recommendations For The Authors):**

(1) *The figures and tables should be substantially improved.*

We thank the reviewer for pointing this out. We have improved some of the figures' quality.

| (2) *Please explain the sample size, and the difference between Schallmo eLife 2018, and Melnick, 2013.*

We thank the reviewer for pointing this out. These questions are answered in the public review. We copy the answer in the public review.

| (2.1) *How was the sample size determined? Is it sufficient??*

Thank you to the reviewer for pointing this out. We use G\*power to determine our sample size. In the study by Melnick (2013), they reported a medium effect between SI and Perception Reasoning sub-ability ( $r=0.47$ ). Here we use this  $r$  value as the correlation coefficient ( $p H1$ ), setting the power at the commonly used threshold of 0.8 and the alpha error probability at 0.05. The required sample size is calculated to be 26. This ensures that our study has adequate power to yield valid statistical results. Furthermore, compared to earlier within-subject studies like Schallmo et al.'s 2018 research, which used 22 subjects to examine GABA levels in MT+ and the early visual cortex (EVC), our study includes an enough dataset.

| (2.2) *In Schallmo elife 2018, there was no correlation between GABA concentration and SI. How can we justify the different results different here?*

Thank you to the reviewer for pointing this out. There are several differences between the two studies, ours and theirs:

a. While the earlier study by Schallmo et al. (2018) employed 3T MRS, we utilize 7T MRS, enhancing our ability to detect and measure GABA with greater accuracy.

b. Schallmo elife 2018 choose to use the bilateral hMT+ as the MRS measurement region while we use the left hMT+. The reason why we focus on left hMT+ are described in review 1. (6). Briefly, use of left MT/V5 as a target was motivated by studies demonstrating that left MT/V5 TMS is more effective at causing perceptual effects (Tadin et al., 2011).

c. The resolution of MRS sequence in Schallmo elife 2018 is 3 cm isotropic voxel, while we apply 2 cm isotropic voxel. This helps us more precisely locate hMT+ and exclude more white matter signal.

*(3) Table 1 and Table Supplementary 1-3 contain many correlation results. But what are the main points of these values? Which values do the authors want to highlight? Why are only p-values shown with significance symbols in Table Supplementary 2?*

*(3.1) what are the main points of these values?*

Thank you to the reviewer for pointing this out. These correlations represent the relationship between behavior task (SI/BDT) and resting-state functional connectivity. It indicates that left hMT+ is involved in the efficient information integration network when it comes to the BDT task. In addition, left hMT+'s surround suppression is involved in several hMT+ - frontal connectivity. Furthermore, the overlapping regions between two tasks indicate a shared underlying mechanism.

*(3.2) Which values do the authors want to highlight?*

Table 1 and Table Supplementary 1-3 present the preliminary analysis results for Table 2 and Table Supplementary 4-6. So, we generally report all value. Conversely, in the Table 2 and Table Supplementary 4-6, we highlight (bold font) indicating the significant correlations survived from multi correlation correction.

*(3.3) Why are only p-values shown with significance symbols in Table Supplementary 2?*

Thank you for pointing this out, it is a mistake. We have revised it and delete the significance symbols.

*(4) Line 27, it is unclear to me what is "the canonical theory".*

We thank the reviewer for pointing this out. We have revised "the canonical theory" to "the prevailing opinion".

*(5) Throughout the paper, the authors use "MT+", I would suggest using "hMT+" to indicate the human MT complex, and to be consistent with the human fMRI literature.*

We thank the reviewer for pointing this out. We have revised them and used "hMT+" to be consistent with the human fMRI literature.

*(6) At the beginning of the results section, I suggest including the total number of subjects. It is confusing what "31/36 in MT+, and 28/36 in V1" means.*

We thank the reviewer for pointing this out. We have included the total number of subjects in the beginning of result section.

*(7) Line 138, "This finding supports the hypothesis that motion perception is associated with neural activity in MT+ area". This sentence is strange because it is a well-established finding in numerous human fMRI papers. I think the authors should be more specific about what this finding implies.*

We thank the reviewer for pointing this out. We have deleted the inappropriate sentence "This finding supports the hypothesis that motion perception is associated with neural activity in MT+ area".

*(8) There are no unit labels for all x- and y-axes in Figure 1. I only see the unit for Conc is mmol per kg wet weight.*

We thank the reviewer for pointing this out. Figure 1 is a schematic and workflow chart, so labels for x- and y-axes are not needed. I believe this confusion might pertain to Figure 3. In Figures 3a and 3b, the MRS spectrum does not have a standard y-axis unit as it varies based on the individual physical conditions of the scanner; it is widely accepted that no y-axis unit is used. While the x-axis unit is ppm, which indicate the chemical shift of different metabolites. In Figure 3c, the BDT represents IQ scores, which do not have a standard unit. Similarly, in Figures 3d and 3e, the Suppression Index does not have a standard unit.

*(9) Although the correlations are not significant in Figure Supplement 2&3, please also include the correlation line, 95% confidence interval, and report the r values and p values (i.e., similar format as in Figure 1C).*

We thank the reviewer for pointing this out. We have revised them.

*(10) There is no need to separate different correlation figures into Figure Supplementary 1-4. They can be combined into the same figure.*

We thank the reviewer for the suggestion. However, each correlation figure in the supplementary figures has its own specific topic and conclusion. The correlation figures in Supplementary Figure 1 indicate that GABA in V1 does not show any correlation with BDT and SI, illustrating that inhibition in V1 is unrelated to both 3D visuo-spatial intelligence and motion suppression processing. The correlations in Supplementary Figure 2 indicate that the excitation mechanism, represented by Glutamate concentration, does not contribute to 3D visuo-spatial intelligence in either hMT+ or V1. Supplementary Figure 3 validates our MRS measurements. Supplementary Figure 4 addresses potential concerns regarding the impact of outliers on correlation significance. Even after excluding two “outliers” from Figures 3d and 3e, the correlation results remain stable.

*(11) Line 213, as far as I know, the study (Melnick et al., 2013) is a psychophysical study and did not provide evidence that the spatial suppression effect is associated with MT+.*

We thank the reviewer for pointing this out. It was a mistake to use this reference, and we have revised it accordingly.

*(12) At the beginning of the results, I suggest providing more details about the motion discrimination tasks and the measurement of the BDT.*

We thank the reviewer for pointing this out. We have included some brief description of task at the beginning of the result section.

*(13) Please include the absolute duration thresholds of the small and large sizes of all subjects in Figure 1.*

We thank the reviewer for the suggestion. We have included these results in Figure 3.

*(14) Figure 5 is too small. The items in plot a and b can be barely visible.*

We thank the reviewer for pointing this out. We increase the size and resolution of Figure 5.

**Reviewer #2 (Recommendations For The Authors):**

*Recommendations for improving the writing and presentation.*

*I highly recommend editing the manuscript for readability and the use of the English language. I had significant difficulties following the rationale of the research due to issues with the way language was used.*

We thank the reviewer for pointing this out. We apologize for any shortcomings in our initial presentation. We have invited a native English speaker to revise our manuscript.

<https://doi.org/10.7554/eLife.97545.2.sa0>